Cretaceous Research 46 (2013) 43–58

Contents lists available at ScienceDirect

Cretaceous Research

journal homepage: www.elsevier.com/locate/CretRes

The Mid-Cenomanian Event in southeastern France: Evidence from palaeontological and clay mineralogical data

Fabienne Giraud [a, *], Stéphane Reboulet [b], Jean François Deconinck [c], Mathieu Martinez [c], André Carpentier [b], Clément Bréziat [c]

[a] ISTerre, Université de Grenoble 1, UMR 5275 CNRS, 1381 rue de la piscine, F-38041 Grenoble, France
[b] UMR 5276 CNRS Laboratoire de Géologie de Lyon Terre Planètes Environnement, Université Lyon 1-ENS Lyon, Bâtiment Géode, 2 rue Raphaël Dubois, 69622 Villeurbanne cedex, France
[c] UMR 6282 CNRS, Université de Bourgogne, 6 boulevard Gabriel, 21000 Dijon, France

ARTICLE INFO

Article history:
Received 17 May 2013
Accepted in revised form 6 September 2013
Available online

Keywords:
Calcareous nannofossils
Ammonoids
Primary productivity
Climatic conditions
Middle Cenomanian
Vocontian Basin

ABSTRACT

Reconstruction of main palaeoenvironmental conditions across the Mid-Cenomanian Event (MCE I) in the hemipelagic Tethyan section of Blieux (Southeast France, Vocontian Basin) is proposed. Quantitative analyses of calcareous nannofossil, ammonoid and clay mineral assemblages have been made and compared with respect to sea level changes and the carbon cycle perturbations. The nannofossil primary productivity, as recorded by nannofossil fluxes and relative abundances of meso-eutrophic taxa, is low just below and during the MCE Ia, then slightly increases in the interval including the MCE Ib. The clay assemblages mainly consist of illite/smectite mixed-layers with a smaller proportion of kaolinite. The percentage of kaolinite strongly decreases in the interval including the MCE Ia and slightly increases in the interval including the MCE Ib. The clay assemblages are mainly detrital in origin and reflect environmental changes including differential settling processes, climate, intensity of runoff and detrital sources. The ammonoid assemblages are characterised by a significant change during the MCE I: planispirals (mainly *Schloenbachia*) are dominant until the MCE Ia, whereas heteromorphs (mainly *Sciponoceras*) become dominant from the MCE Ib onwards. Strongly oligotrophic levels in sea surfaces are recorded during the MCE Ia and are related both to arid climatic conditions and major sea level fall (both 3rd order and medium scale lowstand deposits). A decrease in bathymetry could partly explain the decrease in the relative abundance of *Schloenbachia*. The first occurrence of *Sciponoceras* took place during the MCE Ib; this second positive increase in $\delta^{13}C$ is not associated with enhanced nannofossil primary productivity. No clear relations can be established between the occurrence of *Sciponoceras* and trophic resources.

1. Introduction

The Mid-Cenomanian Event (MCE I), first described by Paul et al. (1994), is a carbon-isotope excursion ($\delta^{13}C$) characterised by two positive peaks (MCE Ia, MCE Ib; Mitchell et al., 1996). The MCE I is world-wide and corresponds to a major carbon perturbation recorded in ocean and atmosphere reservoirs as well as in marine carbonates (in England and northern France: Jenkyns et al., 1994; Paul et al., 1994; Mitchell et al., 1996; Jarvis et al., 2001, 2006; southeast France: Reboulet et al., 2013; Spain: Rodriguez-Lazaro et al., 1998; Stoll and Schrag, 2000; Italy: Stoll and Schrag, 2000; northern Germany: Mitchell et al., 1996; Wilmsen, 2007; Morocco: Gertsch et al., 2010; western North Atlantic: Ando et al., 2009), marine organic carbon (tropical Atlantic ocean: Friedrich et al., 2009; Morocco: Gertsch et al., 2010), and terrestrial organic matter (Japan: Uramoto et al., 2007). It is considered to be a prelude to the Oceanic Anoxic Event (OAE) 2, at the Cenomanian/Turonian boundary (Coccioni and Galeotti, 2003), but in contrast to OAE 2, the MCE I is not characterised by the occurrence of black shales (only recognised in the ODP Leg 207, tropical Atlantic Ocean, Demerara Rise; Friedrich et al., 2009; see also synthesis in Reboulet et al., 2013). The MCE Ia and MCE Ib are associated with rapid sea level changes, possibly of glacio-eustatic origin (Gale et al., 2002, 2008). The glaciation hypothesis has been advanced by Stoll and Schrag (2000) and Miller et al. (2003, 2005).

Several authors have suggested a cool climate mode in Western Europe during the MCE I, supported by two southward incursions of boreal nektonic and benthic taxa into European shelf seas which

* Corresponding author.
E-mail address: Fabienne.Giraud-Guillot@ujf-grenoble.fr (F. Giraud).

0195-6671/$ – see front matter © 2013 Elsevier Ltd. All rights reserved.
http://dx.doi.org/10.1016/j.cretres.2013.09.004

occur at the onset of the first carbon-isotope excursion and within the $\delta^{13}C$ maximum of the second excursion, respectively (Paul et al., 1994; Gale 1995; Wilmsen, 2003). On the basis of brachiopod oxygen-isotope data, Voigt et al. (2004) have demonstrated that a cooling event (2–3 °C) coincides with the MCE I on European shelves. However, recent stable isotope data from the tropical and western North Atlantic argue against a mid-Cenomanian glaciation event (Moriya et al., 2007; Ando et al., 2009). This event is also characterised by changes in planktonic, nektonic and benthic assemblages (Paul et al., 1994; Erbacher et al., 1996; Mitchell and Carr, 1998; Rodriguez-Lazaro et al., 1998; Coccioni and Galeotti, 2003; Wilmsen et al., 2005, 2007; Hardas et al., 2012; Friedrich et al., 2009), but the interpretations of these changes are contradictory.

The benthic foraminiferal record suggests that the MCE I was associated in many settings with dysaerobia of lower-intermediate water masses (Basque Basin, Spain; Rodriguez-Lazaro et al., 1998), decreased ventilation on the sea floor (Umbria–Marche Basin, Italy, Coccioni and Galeotti, 2003) or stratification of the water column (Anglo–Paris Basin, Mitchell and Carr, 1998; tropical Atlantic ocean, Friedrich et al., 2009; Hardas et al., 2012). On the contrary, Paul et al. (1994) did not observe any change in the benthic foraminiferal assemblage for the Anglo–Paris Basin. The MCE I was interpreted by some authors as an event of increased marine primary productivity (Umbria–Marche Basin: Erbacher and Thurow, 1997; Coccioni and Galeotti, 2003; Stoll and Schrag, 2001; northern Germany: Wilmsen, 2003). By contrast, in the tropical Atlantic Ocean, lower nutrient concentrations of surface waters affect nannofossil communities and tend to favour oligotrophic surface-dwellers or deep-dwellers (Hardas et al., 2012). In the Basque Basin, the composition of planktonic foraminifera did not change during the MCE I (Rodriguez-Lazaro et al., 1998).

The carbon isotope record suggests that the MCE I was a global event; but the contradictory interpretations in terms of biological changes from different settings suggest that local changes could prevail over global changes. The different sections studied for biological changes, and in particular the pelagic sections are generally very condensed with uniform lithologies. In addition, the biostratigraphic and chemostratigraphic frameworks realised on these sections are not precise enough to allow good correlations with North-West Europe. This could partly explain different results in terms of biological changes observed between the studied settings.

The aim of the present work is to depict the main palaeoenvironmental conditions prevailing across the MCE I in the hemipelagic Tethyan section of Blieux (southeast France, Vocontian Basin, Fig. 1), for which the MCE I has been identified by an integrated stratigraphy and compared precisely with boreal basins (Reboulet et al., 2013). Variations in calcareous nannofossil, ammonoid and clay mineral assemblages were analysed and compared with respect to the carbon cycle perturbation and sea level changes. The results are integrated in a regional-global context.

The Blieux section was previously studied for the palaeoenvironmental characterisation of the Oceanic Anoxic Event 1d (Breistroffer interval; Giraud et al., 2003; Reboulet et al., 2005).

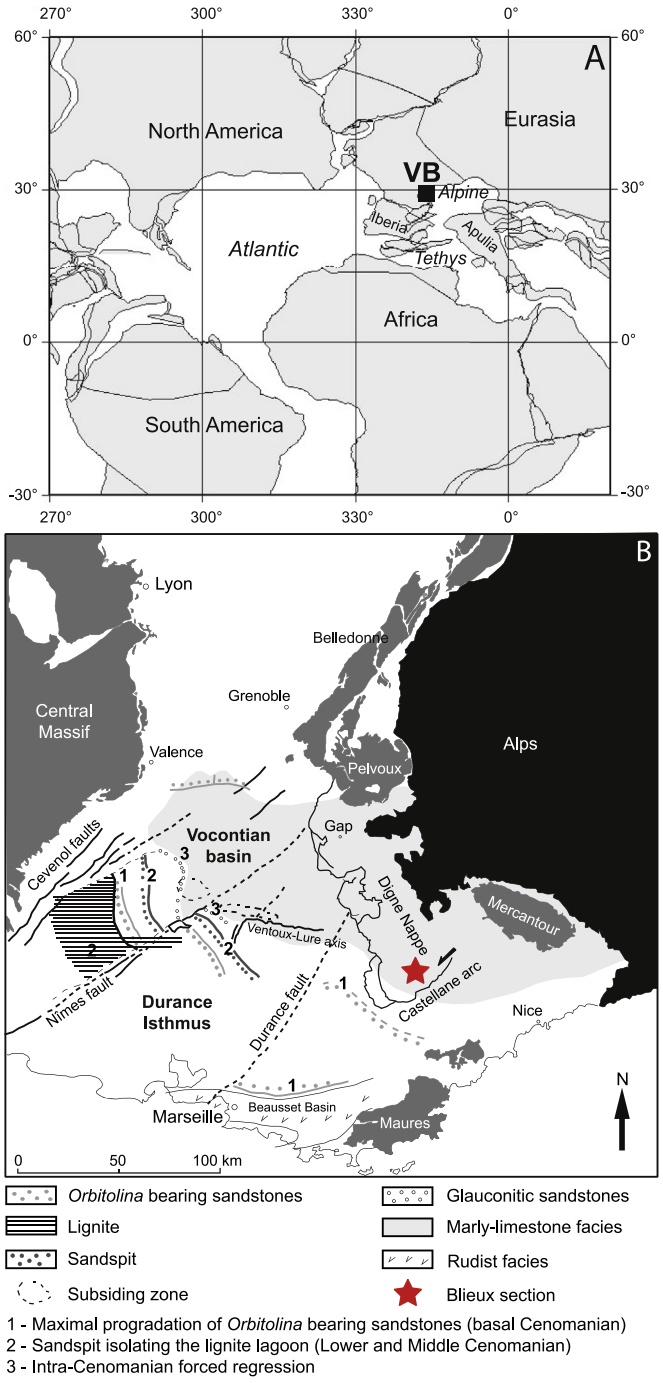

Fig. 1. A. Palaeogeographic map of the western Tethys and Atlantic ocean at 96 My (http://www.adsn.de/odsn/services/paleomap/paleomap.html) with marked position of the Vocontian Basin (VB). **B**. Location of the Blieux section in the Vocontian Basin (Cenomanian palaeogeography modified after Briais (2010)). Abbreviations: VB: Vocontian Basin.

2. Geological setting and stratigraphy

A detailed account of the Vocontian Basin was made in Reboulet et al. (2013; and references therein). In this area, during the Albian, the tectonic regime changed from extensional to compressional (Rubino, 1989; Kandel, 1992). An uplift of all the basin margins occurred and was responsible for the emergence of the Durance Isthmus, south of the Provence platform (Masse and Philip, 1976). Thus, a strong differential subsidence took place between the Provence carbonate shelf to the south, with carbonate (rudist-bearing, Philip, 1978) and siliciclastic facies, and the Vocontian Basin to the north, with limestone–marl alternations, corresponding to hemipelagic to pelagic sediments (Conard, 1983). The Blieux section, located in the southeastern part of the Vocontian Basin, is in a key position to record palaeoenvironmental changes between proximal areas (platform environments) and the pelagic realm (open marine water column).

An integrated stratigraphy of the Cenomanian using bio-sequence- and chemo-stratigraphy was realised in the Blieux

section (Reboulet et al., 2013). The Lower and the Middle Cenomanian have been characterised with the identification of the uppermost part of the *Mantelliceras mantelli*, the whole of the *Mantelliceras dixoni* and the lower part of the *Acanthoceras rhotomagense* ammonite zones. The boundary between these two substages has been placed at the appearance of the first *Cunningtoniceras* (*C. cunningtoni*, layer 528; Fig. 2), and lies within the nannofossil Subzone UC2C of Burnett et al. (1998; Fig. 2). The section is represented by alternating thick marly interbeds and thin silty or sandy limestone beds, including locally silty levels interpreted as turbidites, and slumps. These limestone–marl alternations are organised in 5 calcareous bundles separated by large marly intervals. The sequence-stratigraphic analysis allowed two orders of depositional sequences to be recognised (medium-scale: 400 ky and large-scale: third order). Just above the Lower/Middle Cenomanian boundary, the MCE Ia was identified, corresponding to a positive excursion of $\delta^{13}C$ (+0.6‰; lowermost part of the *A. rhotomagense* Zone). A second increase (+1.1‰) showing a plateau rather a peak, is recorded and corresponds to the MCE Ib. The duration of the MCE I was estimated to be less than 400 ky. The integrated study of Reboulet et al. (2013) allowed the correlation of the Tethyan Blieux section with boreal sections (Anglo–Paris and Lower Saxony basins). The present work focuses on the stratigraphic interval from the base of the calcareous bundle 3 to the top of bundle 5, including the MCE I (Fig. 2).

3. Material and methods

3.1. Calcimetry and calcareous nannofossils

Calcium carbonate content was determined using the carbonate bomb technique, which measures CO_2 emission during a hydrochloric acid attack. The $CaCO_3$% was calculated using equations presented in Peybernes et al. (2013).

Samples for nannofossil studies were prepared using the random settling technique of Geisen et al. (1999), a method adapted from Beaufort (1991) allowing the calculation of absolute abundances. Nannofossils were observed under a light polarising microscope, at 1560× magnification. The taxonomic frameworks of Perch-Nielsen (1985) and Burnett et al. (1998) are followed. The nannofossil preservation was evaluated following the classes defined by Roth (1983). For the quantification of nannofossils, 300 specimens were counted in a variable number of fields of view on the smear slide in the richest samples. In the poorest samples, specimens were counted following one longitudinal transverse (200 fields of view). Relative abundance of each species was also calculated in each sample. Nannofossil absolute abundances are usually biased by dilution. Therefore, nannofossil fluxes were calculated, using estimation of duration of the succession based on cyclostratigraphy calibration made at Blieux (Reboulet et al., 2013). The sedimentation rates were calculated for the intervals corresponding to the medium-scale sequences of 400 ky eccentricity cycles (Reboulet et al., 2013; Fig. 2). The nannofossil fluxes are expressed as *F* (number of nannofossils per meter square and per year) = "*AA* × *r* × sed. rate" with *AA* = nannofossil absolute abundance; *r* = volume mass of calcite (2.7 g cm^{-3}) and sed. rate = sedimentation rate.

The composition of nannofossil assemblages is also described by the species richness, the Shannon Diversity Index and evenness which are defined by Shannon and Weaver (1949).

The relationships between the different palaeoenvironmental proxies ($CaCO_3$%, nannofossil absolute abundance and flux, species richness, diversity, evenness and relative abundances of some selected nannofossil taxa) were investigated by linear correlation (Correlation coefficient of Pearson). The data set was composed of 40 samples. We used all species or group of species representing more than 1% of the total assemblage. Since some species or groups present low relative abundance compared to the others, the percentages were normalised following an angular transformation or arcsin transformation (Sokal and Rohlf, 1995). The angular transformation allows the normalisation of the lowest and the highest percentages (<5% or >95%). The correlation coefficient of Pearson can be used only with variables showing a Gaussian distribution. To answer to this criterion, the nannofossil absolute abundance and flux were normalised, in calculating the $\log arithm_{10}$ of each absolute abundance or flux value. For each correlation coefficient, a statistical test for significance was computed.

3.2. Ammonoids

The sampling of macrofaunal assemblages was carried out at 37 layers, from layers 494 to 648 of the Blieux section (Fig. 2). The marly intervals were not sampled as the outcrop conditions are less favourable. In total, 301 ammonoids were found in the selected interval and 285 specimens have been taxonomically identified. Dissolution of shells is the norm and specimens are preserved as internal calcareous moulds. Their fragmentation is relatively frequent and compaction is important, particularly for the phragmocone. Consequently, the identification of ammonoids at specific level is often difficult or impossible and data are here presented at the generic level (specimens identified with doubt are indicated by a question mark). This also avoids problems related to the systematics. Cecca (1998) emphasised that it would be preferable to work at the generic level for palaeoecological studies. The Cenomanian ammonoid fauna of the studied interval consists of fourteen genera grouped into eleven families and seven super-families, using the classification proposed by Wright et al. (1996) and emended by Klein et al. (2009) for Phylloceratoidea (see Appendix in Reboulet et al., 2013). The palaeontological study of ammonoids was started by Carpentier (2007) and was reviewed and completed by Reboulet et al., (2013). Genera are here assigned to six morphologic units using the terminology proposed in the glossary of the "Ammonoid Paleobiology" (Landman et al., 1996): involute/evolute planispirals ("normal" coiling) including *Mantelliceras*, *Acanthoceras*, *Cunningtoniceras*, *Schloenbachia*, *Hyphoplites*, *Puzosia (Puzosia)*, *Hyporbulites* and *Tetragonites*; scaphitocones (*Scaphites*); torticones with *Mesoturrilites* and *Turrilites*; orthocones (*Sciponoceras*); ancylocones (*Anisoceras*) and hamitocones (*Hamites*). As the number of specimens per layer is generally low for most of the taxa (8 on average per layer), pie-charts showing the average compositions of ammonoid assemblages are presented for the three intervals (494–516; 518a–548; 578–648) of sampling that nearly correspond to bundles 3–5.

3.3. Clay mineral assemblages

Clay minerals were routinely identified by X-ray diffraction (XRD) on oriented mounts of non-calcareous clay-sized particles (<2 μm), following the analytical procedure of Moore and Reynolds (1997). After removing carbonate using 0.2 N HCl, defloculation of clays was done by successive washing with distilled water. Particles finer than 2 μm were concentrated by centrifugation. Diffractograms were obtained using a Bruker D4 Endeavor diffractometer with CuKα radiations, LynxEye detector and Ni filter, under 40 kV voltage and 25 mA intensity. Three XRD runs were performed, respectively after air-drying, ethylene–glycol solvation, and heating at 490 °C during 2 h. The goniometer performed a scan from 2.5° to 28.5° 2Θ for each run. Identification and semi-quantitative estimates of clay minerals were made according to the position

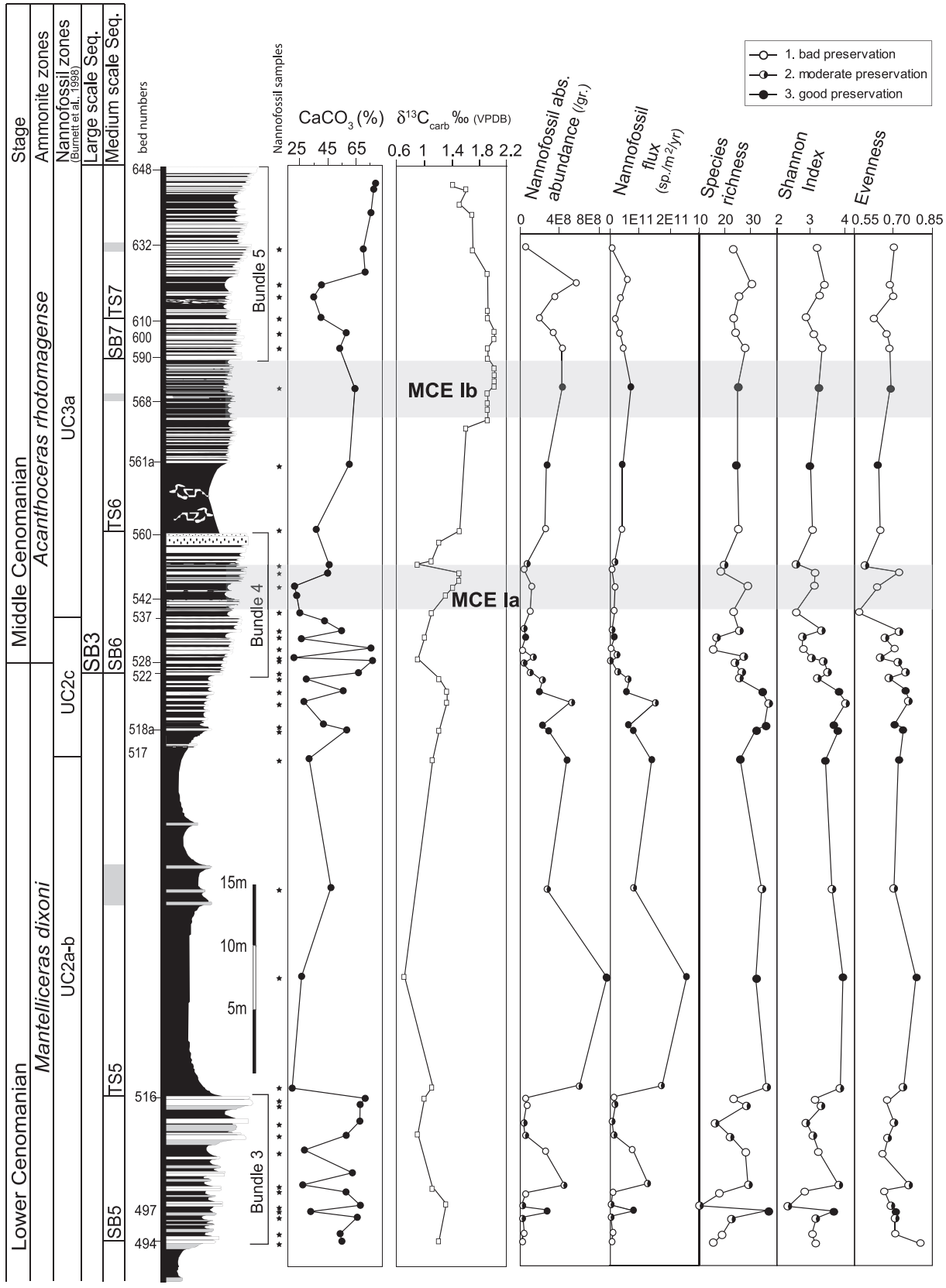

Fig. 2. Stratigraphic changes in calcium carbonate content, carbon-isotope calcareous nannofossil total absolute abundance and flux, species richness, Shannon Index and evenness for the Blieux section. Position of samples is indicated by a small star. Abbreviations: Seq: sequence; SB: sequence boundary; TS: transgressive surface.

and the area of the (001) basal reflections on the three XRD (Moore and Reynolds, 1997).

4. Results

4.1. Calcimetry and calcareous nannofossils

The range of the carbonate content varies from 24.7 to 72.6%, increasing toward the top of the section (Fig. 2).

All nannofossil taxa observed in the studied section are reported in Appendix A. Supplementary data of Reboulet et al. (2013; http://dx.doi.org/10.1016/j.cretres.2012.06.006.). Preservation of nannofossils is poor to well-preserved (Figs. 2 and 3). Only one sample (543b) presents strongly etched and overgrown nannofossils (E3 and O3).

The nannofossil absolute abundances present highest values in the marly interval between bundles 3 and 4, then decrease dramatically within bundle 4 and show a slight increase in the top of the succession (Fig. 2). Nannofossil fluxes, species richness, diversity and evenness follow the same trends as absolute abundances (Fig. 2). They are generally lower in marly limestones with respect to argillaceous marls. The coccoliths significantly contributing to the nannofossil assemblage (more than 85%) are in decreasing order of abundance: *Watznaueria barnesiae*, *Biscutum ellipticum*, *Prediscosphaera* spp. (*P. cretacea*, *P. ponticula*), *Tranolithus orionatus*, *Rhagodiscus achlyostaurion*, *Eiffelithus turriseiffelii*, small *Zeugrhabdotus* (*Z. erectus* + *Zeugrhabdotus* with major axis smaller than 5 μm) and *Cretarhabdus* spp. (including all species of the genera *Cretarhabdus* and *Retecapsa*; Roth and Krumbach, 1986), *Zeugrhabdotus bicrescenticus*, *Watznaueria communis* and *Zeugrhabdotus noeliae* are frequent. Holococcoliths are also present.

The absolute abundance of *Watznaueria barnesiae* decreases within bundle 4, and strongly increases in the upper part of the succession with highest values recorded (Fig. 3). *W. barnesiae* is dominant in the nannofossil assemblages and percentages fluctuate from 19 to 57.6% with a mean value of 40.2% (Fig. 3). *W. barnesiae* generally presents opposite patterns for the absolute and relative abundances. For instance, its percentage increases within bundle 4 whereas its absolute abundance decreases. The opposite pattern between absolute and relative abundances can be explained by the closed-sum effect. The increase in the percentage of *W. barnesiae* within bundle 4 is linked to the decrease in the percentages of the other taxa.

The absolute abundances of *Biscutum ellipticum* and of small *Zeugrhabdotus* increase in the lower part of the section above bundle 3, then decrease to reach the lowest values within bundle 4 and stay low in the upper part of the succession (Fig. 3). Relative abundances vary from 0.6 to 16% and from 0 to 7%, respectively, with highest values recorded within the marly interval located between bundles 3 and 4. They display an opposite trend with respect to the percentages of *W. barnesiae* (Fig. 3).

The absolute abundances of *Prediscosphaera* spp., *Eiffelithus turriseiffellii* and *Cretarhabdus* spp. follow the same trend as the total nannofossil absolute abundances (Fig. 3). Relative abundances of these three taxa fluctuate from 0 to 16.3%, 0 to 11%, 0 to 5.2%, respectively, with higher percentages generally observed within bundles with respect to marly intervals (Fig. 3).

Lower absolute abundances of *Tranolithus orionatus* are recorded within bundles 3 and 4 with respect to the rest of the succession, and highest values in the marly interval located between bundles 3 and 4 (Fig. 3). Percentages fluctuate from 0 to 14.6% and the highest values are recorded just below and at the base of bundle 4 (Fig. 3).

The absolute abundance of *Rhagodiscus achlyostaurion* is characterised by three peaks: one in the marly interval located in the lower part of the section, a second at the base of bundle 4, and a third with highest values at the top of the succession (Fig. 3). Relative abundances are comprised between 0 and 12% with high values recorded within bundles and maxima at the base of bundle 3 (Fig. 3).

The absolute abundances of *Zeugrhabdotus bicrescenticus* present high values at the base of bundle 3, just above it, and then just below and at the base of bundle 5 (Fig. 3). Relative abundances range from 0 to 5.9% with a maximum at the base of the section, and do not present strong fluctuations (Fig. 3).

Watznaueria communis is not present in the marly interval located between bundles 3 and 4, and presents only one peak in absolute abundance just below bundle 4 (Fig. 3). Percentages fluctuate from 0 to 3.2% and reach a maximum in the upper part of bundle 3 and within bundle 4 (Fig. 3).

The absolute abundances of *Zeugrhabdotus noeliae* are generally higher in the marly interval between bundles 3 and 4 with respect to the rest of the succession whereas the relative abundances, comprising between 0 and 4.3%, present one peak at the base of bundle 3, then decrease and show another peak just above bundle 4 (Fig. 3).

The correlation indices between distinctive variables are shown in Table 1. Several variables show highly significant (N99.9%) negative or positive pairings.

4.2. Ammonoids

The Lower–Middle Cenomanian transition (*Mantelliceras dixoni* Zone *pro parte*) and the lowermost part of the Middle Cenomanian (*Acanthoceras rhotomagense* Zone *pro parte*) of the Blieux section are characterised by a change in the ammonoid fauna (Fig. 4). The ammonoid assemblages are mainly composed of planispirals in bundles 3 (91.8%) and 4 (88.1%) and of heteromorphs in bundle 5 (52.5%). Among planispirals, *Schloenbachia* (Hoplitoidea, Schloenbachiidae) is the dominant genus in bundles 3 (84.9%) and 4 (71.2%) and it declines in bundle 5 (35%). *Hyphoplites* (Hoplitoidea, Hoplitidae) are rare in bundle 3 (2.1 %) and absent in bundles 4 and 5. The relative abundance of *Mantelliceras* (Acanthoceratoidea, Acanthoceratidae) is low in bundle 3 (2.7%). This genus disappears in bundle 4 where the (super)family is represented by *Cunningtoniceras* (15.3%) and *Acanthoceras* (1.7%). Only *Acanthoceras* is present in bundle 5 (10%). From bundles 3 to 5, other planispirals, *Puzosia* (Desmoceratoidea), *Hyporbulites* (Phylloceratoidea) and *Tetragonites* (Tetragonitoidea) are rare or absent (from 0% to 2.5%). The percentage of heteromorphs is low in bundles 3 (8.2%) and 4 (11.9%) where this group is mainly represented by *Scaphites* (Scaphitoidea, Scaphitidae) and *Turrilites* (Turrilitoidea, Turrilitidae). An important change is observed in bundle 5 in which *Sciponoceras* (Turrilitoidea, Baculitidae) is the dominant genus (43.8%). From bundles 3 to 5, other heteromorphs (*Hamites* and *Anisoceras*) are rare (from 0% to 3.8%).

4.3. Clay mineral assemblages

The clay assemblages mainly consist of illite/smectite mixed-layers (I/S) R0 (i.e., containing more than 50% of smectite layers (Środoń, 1984, Moore and Reynolds, 1997)). Their proportion varies from 72 to 97% for an average of 84%. These minerals are associated with lower proportions of illite (3–15%), kaolinite (0–15%) and traces of chlorite (Fig. 5). From the base to the top of the section, the proportions of I/S increase while those of kaolinite decrease. The relative proportions of I/S mixed-layers, illite and kaolinite show clear relationship with the lithology and the sequential organisation. Marly intervals are enriched with kaolinite, while calcareous bundles correspond to kaolinite-depleted intervals. So, there is a

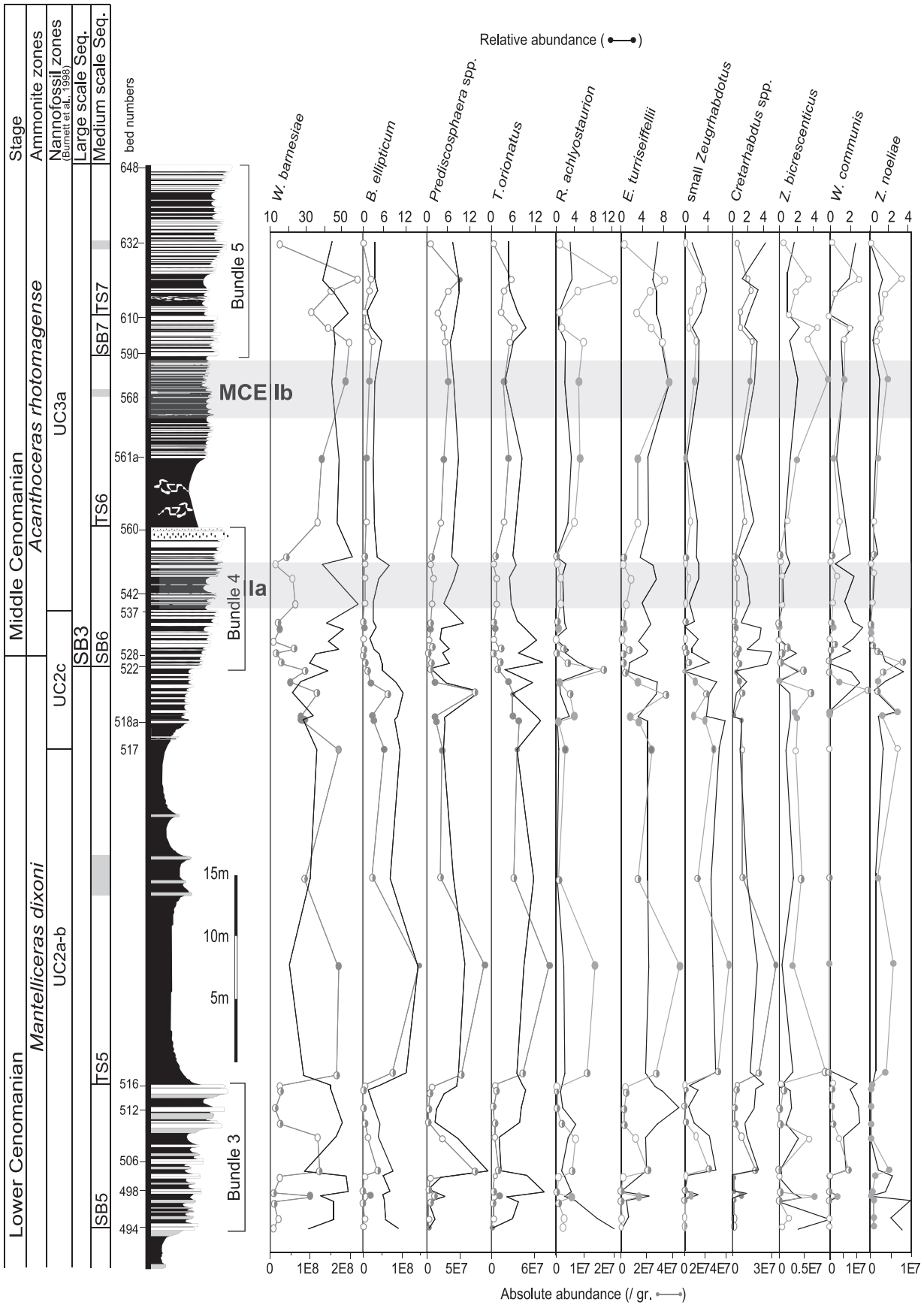

Fig. 3. Absolute and relative abundances of selected calcareous nannofossil taxa for the Blieux section.

Table 1
Correlation analyses between species richness, Shannon Index, evenness, nannofossil absolute abundance and flux, the relative abundance of selected species and calcium carbonate content. The number of measurements is 39. The very poorly-preserved sample 543b, has been excluded from this statistical analysis. The Correlation coefficient of Pearson is in bold where it is statistically significant (p (probability) < 0.05).

	Species richness	Shannon Index	Evenness	Nannofossil abs. abundance	Nannofossil flux	*W. barnesiae* (%)	*B. ellipticum* (%)	*Prediscosphaera* spp. (%)	*T. orionatus* (%)	*R. achlyostaurion* (%)	*E. turriseiffelii* (%)	small *Zeugrhabdotus* (%)	*Cretarhabdus* spp. (%)	*Z. bicrescenticus* (%)	*W. communis* (%)	*Z. noeliae* (%)	$CaCO_3$ (%)
Species richness	1.000																
Shannon Index	**.754**	1.000															
Evenness	.167	**.767**	1.000														
Nannofossil abs. abundance	**.632**	**.626**	.323	1.000													
Nannofossil flux	**.613**	**.720**	.489	**.900**	1.000												
W. barnesiae (%)	−.515	**−.922**	−.557	**−.701**	**.741**	1.000											
B. ellipticum (%)	.259	**.629**	**.726**	.517	**−.775**	**−.775**	1.000										
Prediscosphaera spp. (%)	.525	.417	.084	.536	.457	−.320	.071	1.000									
T. orionatus (%)	−.054	.037	.112	−.136	−.045	−.091	.147	−.253	1.000								
R. achlyostaurion (%)	−.393	−.125	.222	−.251	−.232	−.016	.064	−.488	−.332	1.000							
E. turriseiffellii (%)	.316	.137	−.125	.229	.075	.031	−.299	.423	−.080	**−.604**	1.000						
small *Zeugrhabdotus* (%)	.692	**.731**	.420	**.632**	**.686**	**−.666**	.528	.494	.170	−.454	.212	1.000					
Cretarhabdus spp. (%)	.126	.157	.063	.102	.051	−.092	−.224	.340	.006	−.327	.452	.168	1.000				
Z. bicrescenticus (%)	−.127	−.068	.061	−.070	−.085	.031	−.029	−.262	−.260	.500	−.170	−.237	−.230	1.000			
W. communis (%)	−.006	−.126	−.209	−.185	−.255	.209	.424	.273	−.174	−.323	**.610**	−.191	.393	−.218	1.000		
Z. noeliae (%)	−.239	.008	.258	−.133	−.087	−.124	.254	−.513	.001	**.609**	**−.691**	−.196	−.500	.122	**−.593**	1.000	
$CaCO_3$ (%)	−.453	−.222	.105	−.493	−.516	.123	−.278	−.362	.330	.116	.045	−.333	.102	.105	.092	.171	1.000

clear inverse correlation between the proportions of I/S and kaolinite while there is no clear relationship between I/S or kaolinite with illite, whose proportions vary little. This inverse correlation is particularly well-expressed by the ratio kaolinite / I/S (Fig. 5).

5. Interpretation

5.1. Calcareous nannofossils

5.1.1. Nannofossil preservation

The preservation state can control nannofossil absolute abundance, species richness and diversity, and the relative abundance of some species. With the exclusion of one dissolved sample (543b), the mean nannofossil absolute abundance varies from 1.9 E08 sp./g of rock in poorly-preserved samples to 3.4 E08 sp./g of rock in well-preserved samples. Well-preserved samples contain an average of 31 species, while poorly-preserved samples show a slightly lower mean richness of 25.5. The mean Shannon Index value varies from 3.05 in poorly-preserved samples to 3.45 in well-preserved samples and does not present strong fluctuations. These values reflect assemblages with moderate diversity (Frontier and Pichod-Viale, 1998).

The dissolution susceptibility of main taxa encountered in this study and of other coccoliths characterised by delicate structures are reported in Table 2. *Watznaueria barnesiae* is considered by the different authors as the most resistant Mesozoic placolith to dissolution, while *Biscutum ellipticum*, *Zeugrhabdotus erectus* (including in small *Zeugrhabdotus* group), *Discorhabdus*, *Cretarhabdus surirellus*, *Cribrosphaerella erhenbergerii*, *Helicolithus trabeculatus*, *Prediscosphaera* and *Tranolithus orionatus* are dissolution-susceptible, and a diagenetic overprint may imply an increase in the relative abundance of *W. barnesiae* and a decrease in those of fragile taxa.

For the Blieux section, the relative abundance of *W. barnesiae* displays negative correlation with species richness ($r = -0.515$), Shannon Index ($r = -0.922$), evenness ($r = -0.896$), nannofossil absolute and flux ($r = -0.557$ and $r = -0.701$), and the relative abundance of the delicate species *B. ellipticum* and small *Zeughrabdotus* ($r = -0.775$ and $r = -0.666$). However, the correlations with species richness and nannofossil absolute abundance are statistically not significant (Table 1). The fluctuations of the mean nannofossil absolute abundance, species richness and relative abundances of *W. barnesiae* and dissolution-susceptible taxa have been calculated with respect to the three recognised classes of preservation (Fig. 6). Higher mean absolute abundance, species richness and percentages of delicate taxa and lower mean percentage of *W. barnesiae* are recorded in well-preserved samples (class E1-O1) with respect to the other classes. However, a significant difference is only observed for the mean relative abundance of delicate taxa between poorly- and well-preserved samples. This suggests that the relative abundance of delicate taxa is slightly affected by diagenesis. One of the most remarkable changes in the nannofossil assemblage composition is the overall decrease of the dissolution-susceptible *B. ellipticum* and small *Zeugrhabdotus* across the MCE I. This decline could be interpreted as a diagenetic signal. However, this decline is recorded both in poorly- and well-preserved samples. In addition, through bundle 4 which includes the MCE Ia, both the total nannofossil absolute abundance and the abundance of different taxa decrease, whatever the preservation state. In bundle 5 characterised by poorly-preserved samples, the absolute abundances of the different taxa increase. This indicates that the decrease in nannofossils recorded through bundle 4 is a primary rather a diagenetic signal.

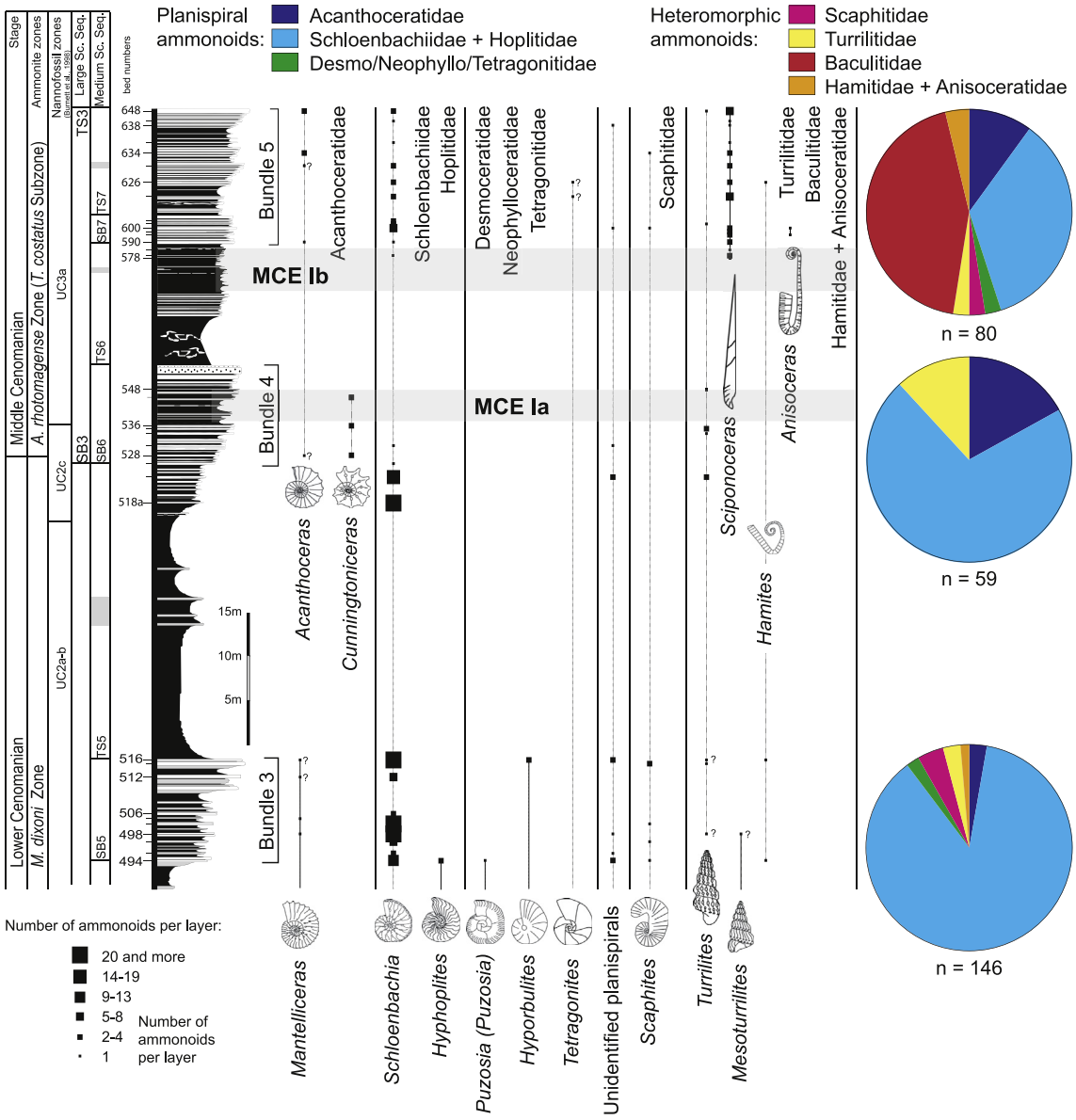

Fig. 4. Stratigraphic distribution of ammonoids at the generic level from layers 494 to 648 of the Blieux section. The average composition of assemblages for three intervals of sampling (494–516; 518a–548; 578–648), that nearly correspond to bundles 3–5, are presented by pie-charts; "*n*" indicates the number of identified specimens for each interval.

The dominance of *Watznaueria* for this time interval seems to be not only the consequence of selective diagenesis but can reflect a primary signal. In the Blieux section, the nannofossil assemblages are generally dominated by *W. barnesiae*. Except in the Middle Cenomanian of the ODP site 1260 (Hardas et al., 2012), *W. barnesiae* is the most abundant or dominant species in poorly- to well-preserved Cenomanian assemblages at different latitudinal and palaeogeographic settings (shallow marine sections of Morocco, Gertsch et al., 2010 and of the southern Carnarvon Platform in western Australia, Howe et al., 2000; mid-shelf area of southern England, Linnert et al., 2011b; intrashelf Lower Saxony Basin, Linnert et al., 2010; hemipelagic sections from the Carpathians, Melinte-Dobrinescu and Bojar, 2008, Vocontian Basin in SE France, Gale et al., 1996; Fernando et al., 2010, and pelagic settings, Dolomites in northern Italy, Luciani and Cobianchi, 1999; Indian ocean, Lees, 2002; Goban Spur, North Atlantic, Linnert et al., 2011a; Demerara Rise, Equatorial Atlantic, Early and Late Cenomanian, Hardas and Mutterlose, 2007).

5.1.2. Nannofossil primary productivity

Variations in nannofossil primary productivity can be estimated with two proxies: the nannofossil flux and the relative abundance of meso-eutrophic nannofossil taxa (*Biscutum ellipticum* and small *Zeugrhabdotus*; Peybernes et al., 2013). In the Blieux section, the nannofossil flux displays a positive correlation with the relative abundance of both *B. ellipticum* and small *Zeugrhabdotus* (Table 1). These taxa are interpreted by different authors as eutrophic or meso-eutrophic taxa (Roth and Bowdler, 1981; Erba et al., 1992; Mutterlose, 1992; Watkins, 1989; Giraud et al., 2003). In the Blieux section, their relative abundance presents positive correlations with species richness, Shannon Index and evenness (Table 1), suggesting that there are more indicative of meso-eutrophic rather than real eutrophic conditions.

In the interval corresponding to bundle 3 which represents part of a 3rd order highstand system deposits (HSD), and a 400 ky lowstand system deposits (LSD), the nannofossil productivity is low. Nannofossil assemblages here are characterised by higher

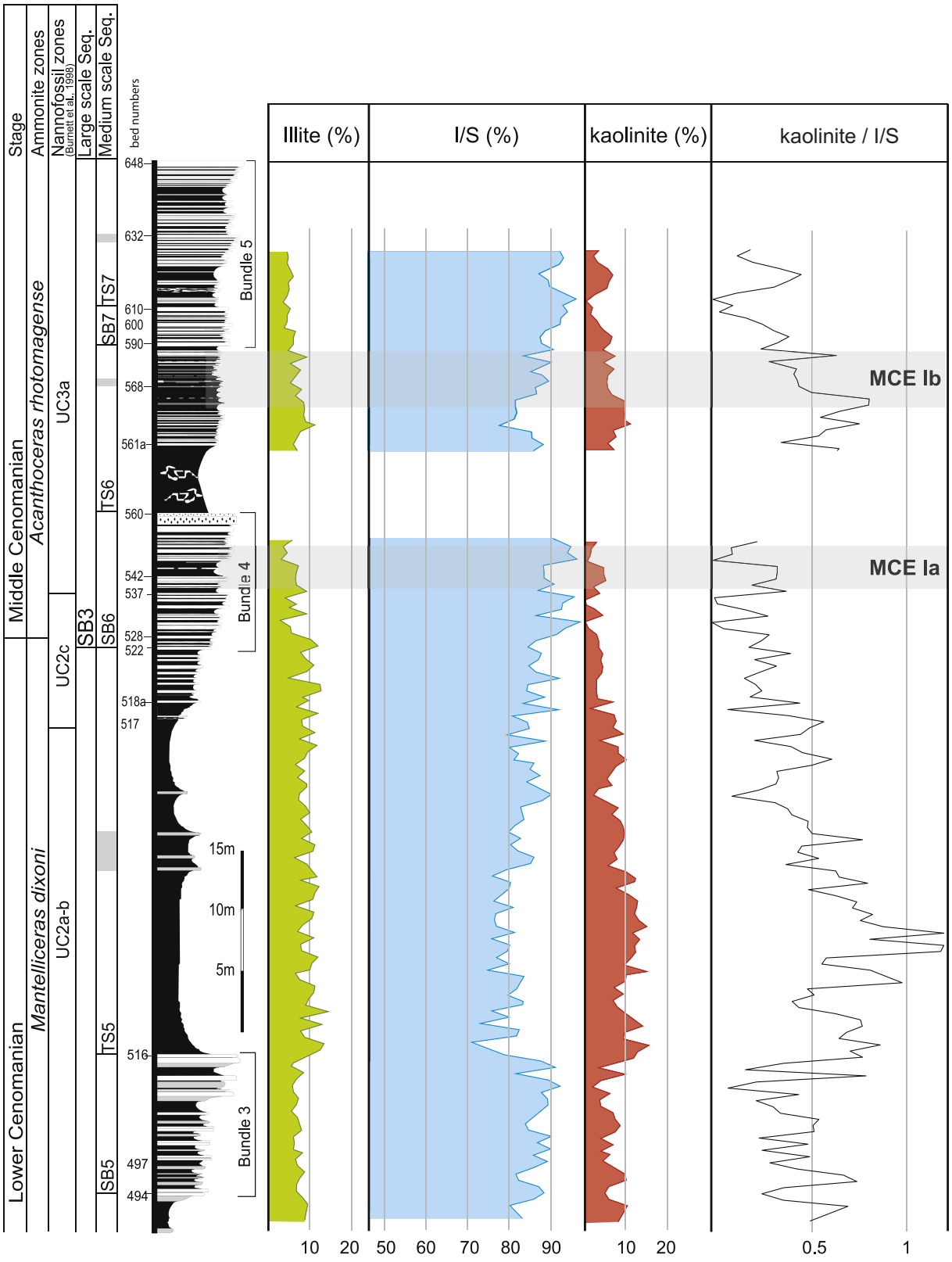

Fig. 5. Clay mineralogy of the Blieux section and kaolinite / I/S ratio.

relative abundances of taxa indicative of oligotrophic conditions such as *Cretarhabdus* spp., *Rhagodiscus achlyostaurion* (Eshet and Almogi-Labin, 1996; Mutterlose, 1996; Mutterlose and Kessels, 2000; Eleson and Bralower, 2005) and taxa without well-defined palaeoecological affinities such as *Zeugrhabdotus noeliae* and *Z. bicrescenticus*. *Prediscosphaera* spp. and *Eiffelithus turriseiffellii* are also common in this interval. Very different palaeoecological affinities (from oligotrophic to eutrophic conditions) have been proposed for these two taxa, (Roth and Krumbach, 1986; Crux, 1991; Erba et al., 1995; Mutterlose and Kessels, 2000; Eleson and

Table 2
Dissolution susceptibility of selected nannofossil taxa encountered in this study. 1 – Hill (1975); 2 – Thierstein (1980); 3 – Roth and Bowdler (1981); 4 – Roth and Krumbach (1986); 5 – Roth (1981).

Taxa	Susceptibility to dissolution
Biscutum constans (=B. ellipticum)	dissolution-susceptible form[1,2,3,4] moderately dissolution-susceptible form[5]
Cretarhabdus crenulatus	moderately dissolution-susceptible form[2] solution-resistant[1]
Cretarhabdus surirellus	dissolution-susceptible form[2]
Cretarhabdus (shields)	solution-resistant[2]
Cretarhabdus spp.	solution-resistant[2,4,5]
Cribrosphaerella erhenbergii	dissolution-susceptible[1,2]
Eiffelithus turriseiffellii	solution-resistant[4] moderately dissolution-susceptible form[1,2]
Discorhabdus rotatorius	dissolution-susceptible[2]
Helicolithus trabeculatus	dissolution-susceptible[1]
Prediscosphaera cretacea	moderately dissolution-susceptible form[4] dissolution-susceptible[1,2]
Prediscosphaera spinosa	dissolution-susceptible[2]
Rhagodiscus asper	dissolution-susceptible[1] moderately dissolution-susceptible form[4] dissolution-resistant[5]
Tranolithus orionatus	dissolution-susceptible[1]
Zeugrhabdotus erectus	dissolution-susceptible form[4,5]
Watznaueria barnesiae	most resistant placolith to dissolution[1,2,3,4,5]

B. ellipticum is considered as a morphotype of *B. constans* (Bornemann and Mutterlose, 2006).

Bralower, 2005; Hardas and Mutterlose, 2007). The relative abundance of *Prediscosphaera* spp. displays low positive correlations with species richness, Shannon Index and nannofossil flux (Table 1) suggesting that it could be interpreted as low mesotrophic. The relative abundance of *E. turriseiffellii* shows negative correlation with the relative abundance of both *R. achlyostaurion* and *Z. noeliae* and positive correlation with the relative abundance of *Watznaueria communis* (Table 1) but it is difficult to propose palaeoecological affinities for this species. In the marly interval located between bundles 3 and 4, the nannofossil productivity increased and reached a maximum as is attested by the highest values recorded both in nannofossil fluxes and in the relative abundances of meso-eutrophic taxa. These highest values are associated with higher nannofossil species richness and diversity, with respect to the preceeding interval, indicative of optimal conditions for the development of nannoplankton. Thus, sea-surface nutrient conditions were meso-eutrophic rather than eutrophic. This interval represents part of a 3rd order HSD, records 400 ky trangressive system deposits (TSD), maximum flooding zone (MFZ) and the lower part of HSD, and thus, certainly corresponds to the highest sea level conditions for this succession during the Lower–Middle Cenomanian interval. This led to the development of a large photic zone where nannofossils could occupy different ecological niches. The most remarkable change in the nannofossil record is the

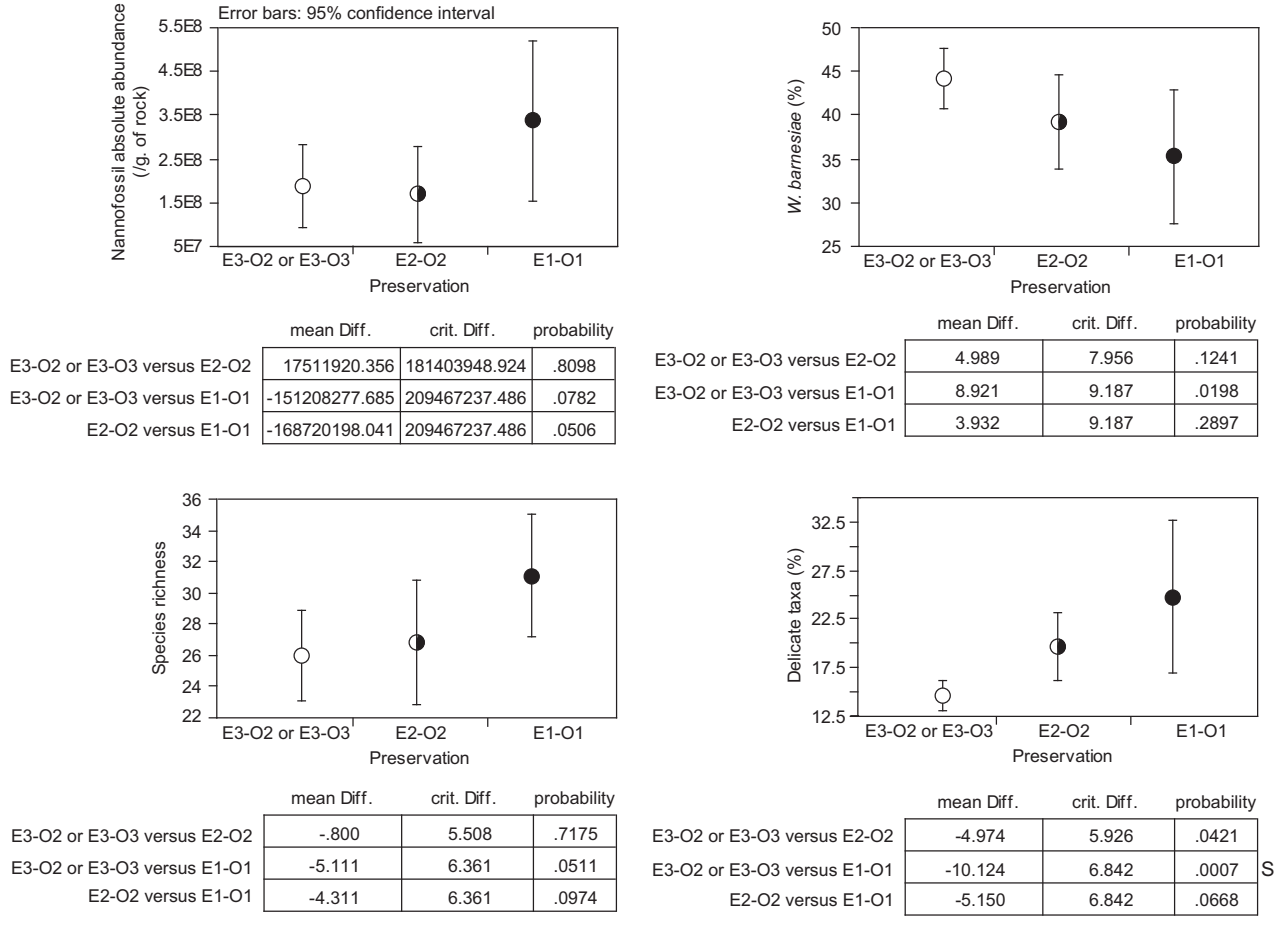

	mean Diff.	crit. Diff.	probability
E3-O2 or E3-O3 versus E2-O2	17511920.356	181403948.924	.8098
E3-O2 or E3-O3 versus E1-O1	-151208277.685	209467237.486	.0782
E2-O2 versus E1-O1	-168720198.041	209467237.486	.0506

	mean Diff.	crit. Diff.	probability
E3-O2 or E3-O3 versus E2-O2	4.989	7.956	.1241
E3-O2 or E3-O3 versus E1-O1	8.921	9.187	.0198
E2-O2 versus E1-O1	3.932	9.187	.2897

	mean Diff.	crit. Diff.	probability
E3-O2 or E3-O3 versus E2-O2	-.800	5.508	.7175
E3-O2 or E3-O3 versus E1-O1	-5.111	6.361	.0511
E2-O2 versus E1-O1	-4.311	6.361	.0974

	mean Diff.	crit. Diff.	probability	
E3-O2 or E3-O3 versus E2-O2	-4.974	5.926	.0421	
E3-O2 or E3-O3 versus E1-O1	-10.124	6.842	.0007	S
E2-O2 versus E1-O1	-5.150	6.842	.0668	

Fig. 6. Mean nannofossil absolute abundance (specimens/gram of rock), mean species richness, mean relative abundance of *Watznaueria barnesiae* and mean relative abundance of susceptible taxa for different classes of preservation for the Blieux section. In order to estimate the significance of the observed differences between the various classes of preservation, a Bonferroni/Dunn test is applied. It allows comparison of the calculated means for datasets with different sizes (here, the highly variable number of samples from one state of preservation to each other). Statistically significant differences were observed at p (probability) <0.0167. Thirty-nine samples are considered in this analysis. Abbreviations: E1-O1: good preservation; E2-02: moderate preservation; E3-O2 or E3-O3: poor preservation; S: significant.

dramatic decrease in productivity and in the assemblage composition (strong decrease in species richness and diversity) recorded below and within bundle 4, including the MCE Ia. The absolute abundances of the main taxa generally decrease during this interval except peaks in absolute abundances of *R. achlyostaurion* and *Z. noeliae*. Strong oligotrophic conditions prevail just below the MCE Ia. These stressful conditions for nannofossils are associated with the maximum regressive conditions recorded in this succession (end of both 3rd order HSD and 400 ky HSD to both 3rd order LSD and 400 ky LSD). Increase in the relative abundance of *T. orionatus* (Roth, 1981; Roth, 1986; Linnert and Mutterlose, 2008) interpreted as a shelf surface waters and/or high-latitude species, can indicate that cooler climatic conditions were associated with the regression. The nannofossil productivity stayed low within the MCE Ia. The recovery of the nannofossil productivity occurred between MCE Ia and Ib, in a 3rd order LSD but during a 400 ky TSD. Low values in absolute and relative abundances of *B. ellipticum* and small *Zeugrhabdotus* and increase in abundances of other main taxa suggest that sea-surface nutrient conditions were meso-oligotrophic rather than really mesotrophic.

In conclusion, in the Blieux section, the MCE I is not associated with a high primary productivity by calcareous nannofossils.

5.2. Ammonoids

The main event in the Cenomanian ammonoid fauna of the Blieux section occurs at the transition between bundles 4 and 5; it is characterised by the decrease of the relative abundance of planispirals (mainly *Schloenbachia*) and the dominance of heteromorphs (mainly *Sciponoceras*, Fig. 4). Thus, the discussion will focus on these genera. The presence *versus* absence of ammonoid taxa (diversity) and their abundance variations can be interpreted in terms of biogeographic affinities of the faunas, palaeoenvironments and palaeoceanographic changes as sea level and/or climatic and/or trophic resource varied. This approach allows a discussion about the various habitats of ammonoids (proximal *versus* distal settings; shallow *versus* deep waters).

Among involute/evolute planispiral ammonoids, *Schloenbachia* is generally the most dominant genus in the Blieux section (Reboulet et al., 2013; Fig. 4). This genus is generally interpreted as belonging to a temperate realm with boreal influence (Juignet and Kennedy, 1976; Kennedy and Cobban, 1976; Thomel, 1992; Monnet and Bucher, 2002; Monnet et al., 2003; Wilmsen and Mosavinia, 2011). During the Cenomanian, Southeast France could have corresponded to the southern boundary of the occidental North European Province as is shown by the distribution and the frequency of the boreal genus *Schloenbachia*.

Thomel (1992) observed that *Schloenbachia* is very abundant in some areas of the Vocontian Basin (see below) in the Lower Cenomanian and in the lower part of the Middle Cenomanian (*A. rhotomagense* Zone; *T. costatus* Subzone); he emphasised that this genus becomes much rarer in the upper part of the *A. rhotomagense* Zone (*T. acutus* Subzone) and it is very rare or even absent at the base of the Upper Cenomanian and through this substage. This trend in abundance variations could be related to the increase in shelf-sea temperatures recorded in several European sections from the lower part of the Middle Cenomanian (top of MCE) to the Cenomanian/Turonian boundary (CTBE) (Voigt et al., 2004). The Middle to Late Cenomanian warming has also been observed in the tropical Atlantic (Demerara Rise, Forster et al., 2007).

The strong abundance of *Schloenbachia* at the Blieux section can be related to the relatively deep palaeoenvironment of the studied area. *Schloenbachia* was generally abundant in pelagic/distal palaeoenvironments and rare in neritic/proximal palaeoenvironments of the Vocontian Basin (Thomel, 1972, 1992). This genus seemed also to be slightly more frequent in distal than in proximal palaeoenvironments of the Anglo–Paris Basin (data of the *A. rhotomagense* Zone; Juignet and Kennedy, 1976). Therefore, *Schloenbachia* could have inhabited the neritic area but they preferentially lived in the open oceanic domain. Taking into account this interpretation, the regression observed around the Lower/Middle Cenomanian boundary (Juignet, 1980; Gale, 1990, 1995; Robaszynski et al., 1998; "The Mid Cenomanian Eustatic Low" of Hancock (2003)) and consequently the decrease in bathymetry during the early part of the Middle Cenomanian (3rd order LSD, Fig. 4) could partly explain the decrease in abundances of *Schloenbachia* and their low number in the lower part of the Middle Cenomanian of the Blieux section.

Among heteromorphs, *Sciponoceras* is the most characteristic genus due to its great abundance in the Middle Cenomanian of the Blieux section where it reaches 43.8% in the assemblages in bundle 5 (Fig. 4). These orthocones (*S. baculoides*) are generally rare or absent in shallow/proximal palaeoenvironments and common or abundant in deep/distal palaeoenvironments of North-West European basins (Juignet and Kennedy, 1976; Kennedy and Cobban, 1976; Thomel, 1992; Wilmsen, 2003; Wilmsen et al., 2007). Taking into account this interpretation about the habitat of *S. baculoides* (that it mainly inhabited in the oceanic domain), the presence *versus* absence of the taxon and its abundance variations during the Cenomanian could be related to sea level variations. This approach is based on a bibliographic compilation concerning the range and abundance of the four successive *Sciponoceras* species (*S. roto*, Robaszynski et al., 1980; Amédro, 1986; Gale et al., 1996, 2011; *S. baculoides*, Reboulet et al., 2013 and references therein; *S. gracile* and *S. bohemicum anterius*, Robaszynski et al., 1998; Gale et al., 2005) in the Anglo–Paris Basin (Kennedy and Juignet, 1975; Kennedy and Juignet, 1983; Robaszynski et al., 1998; Amédro and Robaszynski, 1999) and in the Münster Basin (Wilmsen, 2003; Wilmsen et al., 2007). According to this, it appears that *Sciponoceras* could be present during 3rd order Lowstand System Tract (scattered occurrence) but it generally occurred in mass during 3rd order Transgressive System Tracts. In the Blieux section (Fig. 4), the first *Sciponoceras* occurred in the upper part of 3rd order LSD; no sampling has been made for the uppermost part of the section interpreted as 3rd order TSD.

The Mid-Cenomanian Event I is composed of two peaks, Ia and Ib (Jarvis et al., 2006 and reference therein). In the Anglo–Paris and Lower Saxony basins, the first occurrence of *S. baculoides* is recorded in layers C1 (Southerham, Paul et al., 1994) and C1e (Wunstorf, Wilmsen et al., 2007), characterised by the second peak of the positive $\delta^{13}C$ excursion (MCE Ib; see Reboulet et al., 2013 for correlations). In the other studied sections of these two basins (Reboulet et al., 2013), these orthocones are recorded slightly higher: C5 at Cap Blanc-Nez and Damnes (Amédro et al., 1994; Amédro and Robaszynski, 1999; Robaszynski et al., 1998) and C6 at Folkestone (Paul et al., 1994). This could be explained by local variations in the preservation and/or by the fact that *S. baculoides* is rare in the lower part of its range and common to frequent in the upper part (Reboulet et al., 2013 and references therein). In the Speeton section (Cleveland Basin, England; Paul et al., 1994), *S. baculoides* has been found in one layer: C1 that recorded the second peak of the positive $\delta^{13}C$ excursion. In the Blieux section, *S. baculoides* first occurs in layer 578 that corresponds to the highest value of the second peak (MCE Ib, Reboulet et al., 2013, Fig. 9). An increase in $\delta^{13}C$ recorded in marine carbonate is generally interpreted as the consequence of an increase in primary productivity (sink of light carbon) sometimes associated with an increase in organic matter preservation (Scholle and Arthur, 1980; Arthur et al., 1987). Could there not be a link between the occurrence of *Sciponoceras* and the fertility of sea surface waters?

5.3. Clay mineral assemblages

The presence of large amounts of I/S R0 indicates that the sedimentary series did not undergone significant burial. These minerals are very sensitive to temperature increase and their progressive illitisation takes place as soon as the temperature reaches 70–80 °C (Środoń et al., 2009). Consequently the clay assemblages of the Blieux section are mainly detrital in origin and reflect environmental changes including differential settling processes, climate, intensity of runoff and detrital sources. The weak influence of a thermal diagenesis is confirmed by T_{max} values measured on organic-matter of a few samples. These values, comprised between 419 and 433 °C (Sauvage, 2011), are totally consistent with the presence of I/S R0 (Dellisanti et al., 2010) and indicate that organic matter is immature.

5.3.1. Cenomanian clay sedimentation

In North-West Europe, Cenomanian sediments mainly consist of chalk. The clay fraction of the Cenomanian chalk is also dominantly composed of I/S R0 (highly smectitic minerals) but there is some temporal and spatial variability. In Normandy and in the depocenter of the Paris Basin (chalk 700 boreholes) the proportion of I/S R0 reaches 90% throughout the Cenomanian with very little variation (Deconinck et al., 1991b; Deconinck et al., 2005). In the North of France (Boulonnais area, Cap Blanc Nez section), the Lower Cenomanian chalk shows a clay fraction composed of I/S but in the Middle and Late Cenomanian, illite and kaolinite increase sharply (Deconinck et al., 1991b). This change in clay mineralogy occurring at the transition between *M. dixoni* and *A. rhotomagense* zones probably results from increasing runoff following a tectonic rejuvenation of the Anglo–Brabant Massif. In England, the clay fraction of the Lower chalk (Cenomanian in age) equally shows great differences from one section to another (Morgan-Jones, 1977; Jeans, 2006).

5.3.2. Origin of smectitic minerals

The origin of smectitic minerals in marine sediments is controversial (as extensively discussed by Chamley (1989) and Thiry (2000)). The abundance of these minerals in Cretaceous sediments, notably in those drilled in the Atlantic Ocean, is interpreted differently. Smectitic minerals are considered detrital, arguing on their chemical composition (Al–Fe beidellite) similar to smectites formed in soils, Rare Earth Element (REE) profiles, and strontium isotope composition (Chamley, 1989, p. 336–343). A volcanogenic or authigenic origin of smectitic minerals is also often proposed based on the common occurrence of the paragenesis smectite–opal CT-clinoptilolite. The controversy also results mainly from the difference between smectite-poor continental series and smectite-rich marine coeval sediments. This paradox is tentatively explained by the massive neoformation of smectite in oceanic basins or by the transformation of detrital clay particles into smectitic minerals (Thiry and Jacquin, 1993). The study of transect from proximal areas to the distal part of the basin shows that differential settling processes are partly responsible for the smectite enrichment in (hemi) pelagic environments (e.g., Chamley et al., 1990; Deconinck and Vanderaveroet, 1996). Considering the clay fraction of the chalk, it is clear that smectitic minerals correspond to a mixture of detrital I/S, authigenic lathed smectites preferentially formed in slowly deposited sediments and smectite deriving from the submarine weathering of volcanic glass shards (Deconinck and Chamley, 1995; Jeans, 2006). Environmental conditions during the Late Cretaceous were altogether favourable to largely dominated smectite-rich clay sedimentation: high sea level, low relief on continental areas, more or less arid climate, low sedimentation rate and volcanism expressed by the common occurrences of bentonite layers notably in the Middle and Upper Turonian (Deconinck et al., 1991a; Wray, 1995, 1999; Wray et al., 1995; Godet et al., 2003; Deconinck et al., 2005).

The abundance of smectitic minerals in the Blieux section is therefore consistent with the usual Cenomanian clay sedimentation. The most striking feature observed on the Blieux section is the parallel evolution of the kaolinite / I/S ratio with the evolution from a marly sedimentation to calcareous bundles.

The gradual increase in the proportions of smectitic minerals from marly intervals to calcareous bundles can be interpreted in two ways. It can result either from a progressive deepening of the depositional environment or from a gradual transition from humid to more arid climatic conditions. In fact the deepening of the depositional environment may cause an increase of the proportions of smectitic minerals at the expense of kaolinite due to differential sedimentation of these two mineral species. However, this explanation is not consistent with the sequence-stratigraphic interpretation which considers marly intervals as transgressive and representing highstand systems tracts while calcareous bundles are considered to represent lowstand systems tracts (Reboulet et al., 2013). It is more likely that kaolinite-rich marly intervals were deposited during humid periods favouring runoff while smectite-rich calcareous bundles were deposited during more arid climatic conditions.

6. Discussion

6.1. Palaeoenvironmental and palaeoclimatic reconstructions around the MCE I in the Blieux section

Nannofossil and clay mineral assemblages both allow the reconstruction of sea-surface trophic and palaeoclimatic (in terms of humidity/aridity) conditions prevailing during the Early–Middle Cenomanian in the Blieux section. Nutrients for nannofossils can be delivered from the emerged continents to the basin *via* an intensified runoff, during the development of humid conditions as shown by the increase in kaolinite and illite contents (Moiroud et al., 2012). In the Blieux section, a significant positive correlation ($r = 0.542$) has been observed between the kaolinite / I/S ratio and the nannofossil flux (Fig. 7), suggesting that humid *versus* arid climatic conditions mainly control the nannofossil primary productivity. Isotopic carbon data have been already commented on the paper of Reboulet et al. (2013); they are compared with other data in this present study and integrated in the reconstruction

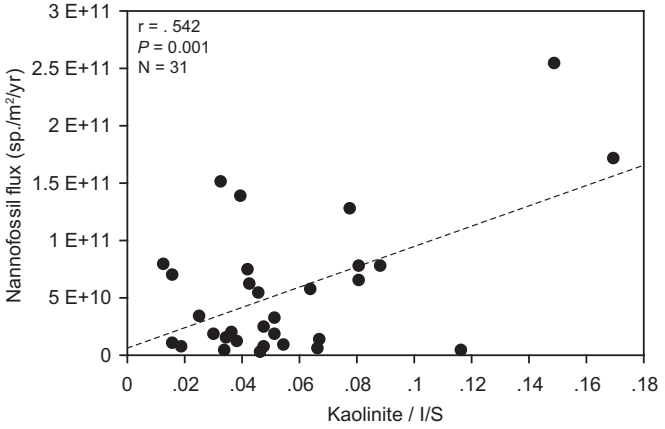

Fig. 7. Bivariate plot showing the relationship between kaolinite / I/S ratio and nannofossil flux. Abbreviations: *r*, coefficient of correlation; *p*, probability; *N*, number of measurements.

when some new interpretations are proposed with respect to the previous work.

In the marly interval located below bundle 4, the nannofossil primary productivity was at a maximum (meso-eutrophic conditions), together with maximum proportions of illite and kaolinite. Nutrients were delivered from the emergent continents to the basin *via* an intensified runoff, during the development of humid conditions. These climatic conditions took place during the end of formation of a 3rd order HSD and 400 ky TSD and HSD.

Just below and within bundle 4, including the MCE Ia, the nannofossil primary productivity decreased to reach very low values (strong oligotrophic conditions). This is compatible with strongly reduced runoff and associated nutrient fluxes due to the development of arid climatic conditions shown by minimum percents of illite and kaolinite. These climatic conditions were contemporaneous with major sea level fall (both 3rd order and 400 ky LSDs). During these palaeoenvironmental conditions (very low nutrient levels and marine regression), there was a reduction in the abundance of nannofossils, ammonoids and benthic macrofauna (sea urchins and inocerams), but no major changes in assemblages are observed in these groups.

In the calcareous interval including the MCE Ib and bundle 5, the nannofossil primary productivity, as recorded by nannofossil fluxes, first increased, then varied with values higher with respect to bundle 4. The abundance of meso-eutrophic nannofossil taxa stayed low during this time interval suggesting low mesotrophic conditions. The MCE Ib occurred at the end of the transgressive part of a medium-scale sequence (400 ky). A larger marine surface can explain an increase in nannofossil productivity, but it can also be due to a return to more humid conditions as indicated by higher illite and kaolinite contents. However, these contents gradually decrease from the MCE 1b interval to the top of bundle 5.

In the Blieux section, the duration of the carbon positive excursion (MCE Ia) and the positive trend (MCE Ib) was estimated to be less than 400 ky; these events have been associated with rapid sea level changes (Reboulet et al., 2013). This interpretation still prevails, since MCE Ia and MCE Ib do not correspond to periods of increasing nutrient influx and associated higher nannofossil primary productivity.

6.2. Nannofossil primary productivity during the Cenomanian

Mean nannofossil flux values of the Blieux section for the Early–Middle Cenomanian interval are reported in Table 3. They are respectively of 6.6 E10 sp./m^2/yr for the Early Cenomanian, 2.58 E10 sp./m^2/yr for the Middle Cenomanian and 3.18 E10 sp./m^2/yr for the interval corresponding to the MCE I. For this time interval, nannofossil absolute abundances (obtained with the same random settling as in the present study) are available for the Lower Saxony Basin (Wunstorf core, Linnert et al., 2010), the DSDP Site 549 (Goban Spur, North Atlantic; Linnert et al., 2011a) and the ODP sites 1260 and 1258 (Demerara Rise, Central Atlantic; Hardas and Mutterlose, 2007 and Hardas et al., 2012). From these values and sedimentation rates calculated from orbital time scale published in Voigt et al. (2008), mean nannofossil fluxes have been calculated (Table 3). The decrease in nannofossil productivity observed in the Blieux section during the MCE I has been recorded in the ODP site 1260 (Hardas et al., 2012). Reduced surface water fertility attested by decrease in the relative abundance of high fertility nannofossil taxa is also observed throughout the OAE 2-interval (or CTBE characterised by two positive peaks in the $\delta^{13}C$) in many locations of Tethys and Atlantic (Linnert et al., 2011a and references herein). Considering the spatial and not temporal variations of nannofossil fluxes, it appears that, the values are not strongly different between the different locations for each interval considered (Early, Middle Cenomanian and MCE I; Table 3). This suggests that sea-surface trophic conditions were more or less similar between the pelagic sites of the Atlantic, the epicontinental settings and the Vocontian Basin. Linnert et al. (2011a and b) have shown that palaeoenvironmental conditions (sea-surface fertility) were very similar between the DSDP site 551 (Goban Spur, North Atlantic) and the Eastbourne section (Anglo–Paris Basin) during OAE 2 times. They interpreted the even distribution of nutrients in marine waters as due to the mode of oceanic circulation, limited to several eddies during the Cenomanian, as was proposed by Hay (2008). This suggests that for each considered time interval (Early, Middle and Late Cenomanian) the distribution of nutrients in marine waters was uniform probably due to the same mode of oceanic circulation. Then, changes in nannofossil productivity during the Cenomanian could be mainly explained by change in climatic conditions.

6.3. The occurrences of Sciponoceras with respect to positive excursions of $\delta^{13}C$

The occurrences of *Sciponoceras* species seem to be correlated with the three major positive $\delta^{13}C$ excursions recognised during the Cenomanian (as previously shown for the Mid-Cenomanian Event I; part 5.2) and its boundaries: Albian/Cenomanian Boundary Event, and Cenomanian/Turonian Boundary Event.

The Albian/Cenomanian Boundary Event (Jarvis et al., 2006) comprised four secondary isotope excursions decreasing in maximum value up section. At the Mont Risou section (SE France), that is the GSSP for base of the Cenomanian Stage (Kennedy et al., 2004), the first occurrence of *S. roto* can be correlated with the fourth peak (named "D" in Gale et al. (1996 and 2011) or "C" in Jarvis et al. (2006)) of the Albian/Cenomanian isotope excursion.

Table 3
Cenomanian nannofossil flux calculated for different palaeogeographical settings, with fruitful collaboration of Baptiste Suchéras-Marx.

	Pelagic setting				Hemipelagic	Intrashelf basin	Mid shelf
	DSDP Site 549 (Goban Spur, North Atlantic)	DSDP Site 551 (Goban Spur, North Atlantic)	ODP Site 1258 (Demerara Rise, Central Atlantic)	ODP Site 1260 (Demerara Rise, Central Atlantic)	Blieux section (Vocontian Basin)	Wunstorf core (Lower Saxony Basin)	Eastbourne section (Anglo–Paris Basin)
Early Cenomanian			1.9 E09 sp./m^2/yr	<4 E10 sp./m^2/yr	6.6 E10 sp./m^2/yr		
Middle Cenomanian	2.6 E10 sp./m^2/yr			<4 E10 sp./m^2/yr	2.58 E10 sp./m^2/yr	2.7 E11 sp./m^2/yr	
MCEI				<1 E10 sp./m^2/yr	3.18 E10 sp./m^2/yr		
Late Cenomanian		7.5 E10 sp./m^2/yr	4.6 E09 sp./m^2/yr	3.6 E10 sp./m^2/yr		1.6 E11 sp./m^2/yr	2.8 E10 sp./m^2/yr
CTBE (OAE 2)		3.7 E10 sp./m^2/yr	5.8 E09 sp./m^2/yr	9.1 E09 sp./m^2/yr		1.3 E11 sp./m^2/yr	2.7 E09 sp./m^2/yr
	Linnert et al. (2011a)	Linnert et al. (2011a)	Hardas and Mutterlose (2007)	Hardas and Mutterlose (2007) Hardas et al. (2012)	this study	Linnert et al. (2010)	Linnert et al. (2011b)

The Cenomanian/Turonian Boundary Event (CTBE) is one of the largest carbon-isotope events in the geological record and is composed of two main build-ups (Jarvis et al., 2006 and references therein). According to the correlations between the Cap Blanc-Nez and Eastbourne sections (Anglo–Paris Basin) established by Robaszynski et al. (1998), the first occurrence of *S. gracile* can be correlated with the first peak of the positive $\delta^{13}C$ excursion taking place in bed 3 of the Plenus Marl Member (*Metoicoceras geslinianum* Zone). In the uppermost part of the *M. geslinianum* Zone of the Eastbourne section (that is used as a reference for the Cenomanian–Turonian succession in the chalk facies of NW Europe; Gale et al., 2005), *S. gracile* is replaced by *S. bohemicum anterius* that first occurs in the second peak of the excursion (first bed of the Ballard Cliff Member). At the Pueblo section (Colorado, USA), the first *S. gracile* has been found in layer 67 that corresponds to the first peak of the positive $\delta^{13}C$ excursion (Gale et al., 2005 and references therein); these authors correlated this layer with bed 3 at Eastbourne.

Positive shifts of $\delta^{13}C$ can be interpreted as enhanced sea surface fertility. A link between trophic resource variations in the water column and the occurrence and/or abundance of heteromorphs has been proposed (Reboulet et al., 2003; Reboulet, 2008). In the Blieux section, calcareous nannofossils do not show a high primary productivity during the MCE I; on the contrary, trophic conditions as recorded by nannofossils were low, and the nannofossil primary productivity cannot explain the positive excursion of $\delta^{13}C$. Moreover, reduced sea-surface fertility, recorded by nannofossils, is also observed for most of the studied sections and DSDP/ODP Sites during the CTBE. Thus, the link between the occurrence of *Sciponoceras* and the positive $\delta^{13}C$ excursions seems to be more complex than a simple interpretation in terms of trophic resources.

7. Conclusions

The analysis of calcareous nannofossils, ammonoids and clay mineral assemblages across the Mid-Cenomanian Event (MCE I) investigated in the Blieux section (southeast France) has led to the following observations.

The highest nannofossil primary productivity occurred in the marly interval located below the MCE I and corresponded to mesotrophic levels in sea surface during humid climatic conditions and 3rd order highstand deposits.

In the calcareous interval (bundle 4) including the MCE Ia, climatic conditions became arid, the nannofossil primary productivity sharply decreased and very oligotrophic levels were recorded in the sea surface. These changes took place during 3rd order and medium scale lowstand deposits. This major sea level fall could partly explain the decrease in the relative abundance of *Schloenbachia* (planispiral ammonoids), that was the dominant genus during the Early Cenomanian.

In the calcareous interval including the MCE Ib and bundle 5, a return to more humid conditions was responsible for increasing runoff and associated nutrients leading to a slight increase in marine nannofossil primary productivity. This interval was characterised by the dominance of *Sciponoceras* (orthocone heteromorph ammonoids). The successive occurrences of *Sciponoceras* during the Cenomanian can be correlated with particular palaeoenvironmental changes: the ranges of the four successive species seem mainly restricted to the third order transgressive system tracts and their first occurrences took place during positive shifts of $\delta^{13}C$. However, in the Blieux section, the positive $\delta^{13}C$ excursion of the MCE I was not explained by an increase in nannofossils primary productivity; consequently no clear relations can be established between the occurrence of *S. baculoides* and trophic resources.

Acknowledgements

The authors are grateful to Professor Peter Rawson (CEMS, University of Hull, Scarborough Campus) for proof reading and correcting the English version of the script, and both reviewers and Marcin Machalski, associate editor of Cretaceous Research, for their constructive comments. This study has been financed by the laboratories UMR 5275 and 5276 of the Universities of Grenoble 1 and Lyon 1. Jean-François Deconinck, Mathieu Martinez and Clément Bréziat were supported by the ANR project ASTS-CM (Astronomical time scale for the Cenozoic and Mesozoic era).

References

Amédro, F., 1986. Biostratigraphie des craies cénomaniennes du Boulonnais par les ammonites. Annales de la Société Géologique du Nord 105, 159–167.
Amédro, F., Colleté, C., Fricot, C., Robaszynski, F., 1994. Extension inter-régionale de niveaux-repères dans les craies cénomaniennes du bassin anglo-parisien (Boulonnais, Aube, Kent). Bulletin d'information des Géologues du Bassin de Paris 31, 3–8.
Amédro, F., Robaszynski, F., 1999. Les craies cénomaniennes du Boulonnais. Comparaison avec l'Aube (France) et le Kent (Royaume Uni). Géologie de la France 2, 33–53.
Ando, A., Huber, B.T., MacLeod, K.G., Ohta, T., Khim, B.-K., 2009. Blake Nose stable isotopic evidence against the mid-Cenomanian glaciation hypothesis. Geology 37, 451–454.
Arthur, M.A., Schlanger, S.O., Jenkyns, H.C., 1987. The Cenomanian-Turonian oceanic anoxic event II, paleoceanographic controls on organic matter production and preservation. In: Brooks, J., Fleet, A. (Eds.), Marine Petroleum Source Rocks, Geological Society of London, Special Publications 24, pp. 399–418.
Beaufort, L., 1991. Adaptation of the random settling method for quantitative studies of calcareous nannofossils. Micropalaeontology 37, 415–418.
Bornemann, A., Mutterlose, J., 2006. Size analyses of the coccolith species *Biscutum constans* and *Watznaueria barnesiae* from the Late Albian "Niveau Breistroffer" (SE France): taxonomic and palaeoecological implications. Geobios 39, 599–615.
Briais, J., 2010. Paléogéographie du bassin du Sud-Est de la France au Crétacé post-Urgonien. Unpublished Master 2. Université Claude Bernard Lyon 1, 51 pp.
Burnett, J.A., Gallagher, L.T., Hampton, M.J., 1998. Upper Cretaceous. In: Bown, P.R. (Ed.), Calcareous nannofossil biostratigraphy, British Micropalaeontological Society Publications Series. Chapman and Hall/Kluwer Academic Publishers, pp. 132–199.
Carpentier, A., 2007. Changements paléocéanographiques au cours du Cénomanien: réponse du plancton calcaire. Unpublished Master 2. Université Claude Bernard Lyon 1, 47 pp.
Cecca, F., 1998. Early Cretaceous (pre-Aptian) ammonites of the Mediterranean Tethys: Palaeoecology and palaeobiogeography. Palaeogeography, Palaeoclimatology, Palaeoecology 138, 305–323.
Chamley, H., 1989. Clay sedimentology. Springer-Verlag, 623 pp.
Chamley, H., Deconinck, J.F., Millot, G., 1990. Sur l'abondance des minéraux smectitiques dans les sédiments marins communs déposés lors des périodes de haut niveau marin du Jurassique supérieur au Paléogène. Comptes Rendus de l'Académie des Sciences Paris 311, 1529–1536.
Coccioni, R., Galeotti, S., 2003. The mid-Cenomanian Event: prelude to OAE 2. Palaeogeography, Palaeoclimatology, Palaeoecology 190, 427–440.
Conard, M., 1983. La dynamique des dépôts cénomaniens de Haute-Provence: observations nouvelles et implications paléogéographiques. Bulletin de la Société Géologique de France 7 (25), 239–246.
Crux, J.A., 1991. Albian calcareous nannofossils from the Gault Clay of Munday's Hill (Bedfordshire, England). Journal of Micropaleontology 10, 203–222.
Deconinck, J.F., Amédro, F., Baudin, F., Godet, A., Pellenard, P., Robaszynski, F., Zimmerlin, I., 2005. Late Cretaceous palaeoenvironments expressed by the clay mineralogy of Cenomanian to Campanian chalks from the East of the Paris Basin (Craie 700 program). Cretaceous Research 26, 171–179.
Deconinck, J.F., Amédro, F., Desprairies, A., Juignet, P., Robaszynski, F., 1991a. Niveaux repères de bentonites d'origine volcanique dans les craies du Turonien supérieur du Boulonnais et de Haute-Normandie. Comptes Rendus de l'Académie des Sciences Paris 312, 897–903.
Deconinck, J.F., Amédro, F., Fiolet-Piette, A., Juignet, P., Renard, M., Robaszynski, F., 1991b. Contrôle paléogéographique de la sédimentation argileuse dans le Cénomanien du Boulonnais et du Pays de Caux. Annales de la Société Géologique du Nord 1 (2ème série), 57–66.
Deconinck, J.F., Chamley, H., 1995. Diversity of smectite origins in Late Cretaceous sediments: example of chalks from northern France. Clay Minerals 30, 365–379.
Deconinck, J.F., Vanderaveroet, P., 1996. Eocene to Pleistocene clay mineral sedimentation off New Jersey, western North Atlantic (sites 903 and 905). In: Mountain, G.S., Miller, K.G., Blum, P., Poag, C.W., Twichell, D.C. (Eds.), Proceedings of the Ocean Drilling Project, Scientific Results 150, pp. 147–170.
Dellisanti, F., Pini, G.A., Baudin, F., 2010. Use of T_{max} as a thermal maturity indicator in orogenic successions and comparison with clay mineral evolution. Clay Minerals 45, 115–130.

Eleson, J.W., Bralower, T.J., 2005. Evidence of changes in surface water temperature and productivity at the Cenomanian/Turonian Boundary. Micropalaeontology 51, 309–334.
Erba, E., Castradori, D., Guasti, G., Ripepe, M., 1992. Calcareous nannofossils and Milankovitvh cycles: the example of the Albian Gault Clay Formation (southern England). Palaeogeography, Palaeoclimatology. Palaeoecology 93, 47–69.
Erba, E., Watkins, D., Mutterlose, J., 1995. Campanian dwarf calcareous nannofossils from Wodejebato Guyot. In: Haggerty, J.A., Premoli-Silva, I., Rack, F., McNutt, M.K. (Eds.), Proceedings of the Ocean Drilling Program, Scientific Results 144, pp. 141–156.
Erbacher, J., Thurow, J., 1997. Influence of oceanic anoxic events on the evolution of mid-Cretaceous radiolaria in the North Atlantic and western Tethys. Marine Micropaleontology 30, 139–158.
Erbacher, J., Thurow, J., Littke, R., 1996. Evolution patterns of radiolaria and organic matter variations: A new approach to identify sea level changes in mid-Cretaceous pelagic environments. Geology 24, 499–502.
Eshet, Y., Almogi-Labin, A., 1996. Calcareous nannofossils as paleoproductivity indicators in Upper Cretaceous organic-rich sequences in Israel. Marine Micropaleontology 29, 37–61.
Fernando, A.G.S., Takashima, R., Nishi, H., Giraud, F., Okada, H., 2010. Calcareous nannofossil biostratigraphy of the Thomel Level (OAE2) in the Lambruisse section, Vocontian Basin, southeast France. Geobios 43, 45–57.
Forster, A., Schouten, S., Bass, M., Sinninghe Damsté, J.S., 2007. Mid-Cretaceous (Albian-Santonian) sea surface temperature record of the tropical Atlantic Ocean. Geology 35, 919–922.
Friedrich, O., Erbacher, J., Wilson, P.A., Moriya, K., Mutterlose, J., 2009. Paleoenvironmental changes across the Mid Cenomanian Event in the tropical Atlantic Ocean (Demerara Rise, ODP Leg 207) inferred from benthic foraminiferal assemblages. Marine Micropaleontology 71, 28–40.
Frontier, S., Pichod-Viale, D., 1998. Ecosystèmes: structure, fonctionnement, évolution. Dunod Paris, 447 pp.
Gale, A.S., 1990. A Milankovitch scale for Cenomanian time. Terra Nova 1, 420–425.
Gale, A.S., 1995. Cyclostratigraphy and correlation of the Cenomanian stage in Western Europe. In: House, M.R., Gale, A.S. (Eds.), Orbital forcing timescales and cyclostratigraphy, Geological Society of London Special Publications 85, pp. 177–197.
Gale, A.S., Hardenbol, J., Hathway, B., Kennedy, W.J., Young, J.R., Phansalkar, V., 2002. Global correlation of Cenomanian (Upper Cretaceous) sequences: Evidence for Milankovitch control on sea level. Geology 30, 291–294.
Gale, A.S., Kennedy, W.J., Burnett, J.A., Caron, M., Kidd, B.E., 1996. The Late Albian to Early Cenomanian succession at Mont Risou near Rosans (Drôme, SE France): an integrated study (ammonites, inoceramids, planktonic foraminifera, nannofossils, oxygen and carbon isotopes). Cretaceous Research 17, 515–606.
Gale, A.S., Kennedy, W.J., Voigt, S., Walaszczyk, I., 2005. Stratigraphy of the Late Cenomanian-Early Turonian Chalk succession at Eastbourne, Sussex, UK: ammonites, inoceramid bivalves and stable carbon isotopes. Cretaceous Research 26, 460–487.
Gale, A.S., Voigt, S., Sageman, B.B., Kennedy, W.J., 2008. Eustatic sea-level record for the Cenomanian (Late Cretaceous) – Extension to the Western Interior Basin, USA. Geology 36, 859–862.
Gale, A.S., Bown, P., Caron, M., Crampton, J., Crowhurst, S.J., Kennedy, W.J., Petrizzo, M.R., Wray, D.S., 2011. The uppermost Middle and Upper Albian succession at the Col de Palluel, Hautes-Alpes, France: An integrated study (ammonites, inoceramid bivalves, planktonic foraminifera, nannofossils, geochemistry, stable oxygen and carbon isotopes, cyclostratigraphy). Cretaceous Research 32, 59–130.
Geisen, M., Bollmann, J., Herrle, J.O., Mutterlose, J., Young, J.R., 1999. Calibration of the random settling technique for calculation of absolute abundances of calcareous nannoplankton. Micropalaeontology 45, 437–442.
Gertsch, B., Adatte, T., Keller, G., Tantawy, A.A.A.M., Berner, Z., Mort, H.P., Fleitmann, D., 2010. Middle and late Cenomanian oceanic anoxic events in shallow and deeper shelf environments of western Morocco. Sedimentology 57, 1430–1462.
Giraud, F., Olivero, D., Baudin, F., Reboulet, S., Pittet, B., Proux, O., 2003. Minor changes in surface water fertility across the Oceanic Anoxic Event 1d (latest Albian, SE France) evidenced by calcareous nannofossils. International Journal of Earth Sciences 92, 267–284.
Godet, A., Deconinck, J.F., Amédro, F., Dron, P., Pellenard, P., Zimmerlin, I., 2003. Enregistrement sédimentaire d'événements volcaniques dans le Turonien du Nord-Ouest du Bassin de Paris. Annales de la Société Géologique du Nord 10, 147–162.
Hancock, J.M., 2003. Lower Sea Levels in the Middle Cenomanian: Notebooks on Geology, Maintenon. Letter 2003/02 (CG2003_L02_JMH) 2003.
Hardas, P., Mutterlose, J., 2007. Calcareous nannofossil assemblages of Oceanic Anoxic Event 2 in the equatorial Atlantic: evidence of an eutrophication event. Marine Micropaleontology 66, 52–69.
Hardas, P., Mutterlose, J., Friedrich, O., Erbacher, J., 2012. The Middle Cenomanian Event in the equatorial Atlantic: the calcareous nannofossil and benthic foraminiferal response. Marine Micropaleontology 96–97, 66–74.
Hay, W.W., 2008. Evolving ideas about the Cretaceous climate and ocean circulation. Cretaceous Research 29, 725–753.
Hill, M.E., 1975. Selective dissolution of mid-Cretaceous (Cenomanian) calcareous nannofossils. Micropalaeontology 21, 227–235.
Howe, R.W., Haig, D.W., Apthorpe, M.C., 2000. Cenomanian-Coniacian transition from siliciclastic to carbonate marine deposition, Giralia Anticline, Southern Carnarvon Platform, Western Australia. Cretaceous Research 21, 517–551.
Jarvis, I., Gale, A.S., Jenkyns, H.C., Pearce, M.A., 2006. Secular variation in Late Cretaceous carbon isotopes: a new $\delta^{13}C$ carbonate reference curve for the Cenomanian-Campanian (99.6–70.6 Ma). Geological Magazine 143, 561–608.
Jarvis, I., Murphy, A.M., Gale, A.S., 2001. Geochemistry of pelagic and hemipelagic carbonates: criteria for identifying systems tracts and sea-level changes. Journal of the Geological Society of London 158, 685–696.
Jeans, C.V., 2006. Clay mineralogy of the Cretaceous strata of the British Isles. Clay Minerals 41, 47–150.
Jenkyns, H.C., Gale, A.S., Corfield, R.M., 1994. Carbon- and oxygen-isotope stratigraphy of the English Chalk and Italian Scaglia and its palaeoclimatic significance. Geological Magazine 131, 1–34.
Juignet, P., 1980. Transgressions-Régressions, variations eustatiques et influences tectoniques de l'Aptien au Maastrichtien dans le Bassin de Paris occidental et sur la bordure du Massif Armoricain. Cretaceous Research 1, 341–357.
Juignet, P., Kennedy, W.J., 1976. Faunes d'Ammonites et biostratigraphie comparée du Cénomanien du nord-ouest de la France (Normandie) et du sud de l'Angleterre. Société Géologique de Normandie et des Amis du Muséum du Havre (éd. Du Muséum du Havre) 63, pp. 1–193.
Kandel, D., 1992. Analyse paléotectonique de la plate-forme méridionale du bassin vocontien et de ses bordures durant l'intervalle barrémo-albien (Ventoux-Lure-Baronnies, chaînes subalpines méridionales, France. Thèse. Université Paris VI, 323 pp.
Kennedy, W.J., Cobban, W.A., 1976. Aspects of ammonite biology, biogeography, and biostratigraphy. The Palaeontological Association, London, Special Papers in Palaeontology 17, 1–94.
Kennedy, W.J., Juignet, P., 1975. Répartition des genres et espèces d'ammonites caractéristiques du Cénomanien du Sud de l'Angleterre et de la Normandie. Comptes Rendus de l'Académie des Sciences Paris 280, 1221–1224.
Kennedy, W.J., Juignet, P., 1983. A Revision of the Ammonite Faunas of the Type Cenomanian. I. Introduction, Ancyloceratina. Cretaceous Research 4, 3–83.
Kennedy, W.J., Gale, A.S., Lees, J.A., Caron, M., 2004. The Global Boundary Stratotype Section and Point (GSSP) for the base of the Cenomanian Stage, Mont Risou, Hautes-Alpes, France. Episodes 27, 21–31.
Klein, J., Hoffmann, R., Joly, B., Shigeta, Y., Vašiček, Z., 2009. Lower Cretaceous Ammonites IV, Boreophylloceratoidea, Phylloceratoidea, Lytoceratoidea, Tetragonitoidea, Haploceratoidea, including the Upper Cretaceous representatives. In: Riegraf, W. (Ed.), Fossilium Catalogus I: Animalia. Backhuys Publishers (Leiden), part 146, pp. 1–416.
Landman, N.H., Tanabe, K., Davis, R.A., 1996. Glossary: Ammonoid Paleobiology. In: Topics in Geobiology Volume 13. Plenum Press, New York, pp. 825–843.
Lees, J.A., 2002. Calcareous nannofossil biogeography illustrates palaeoclimate change in the Late Cretaceous Indian Ocean. Cretaceous Research 23, 537–634.
Linnert, C., Mutterlose, J., 2008. Kalkige Nannofossilien des Untercampans (Oberkreide) von Buldern (Stadt Dülmen; NRW). Geologie Paläontologie Westfalen 71, 77–101.
Linnert, C., Mutterlose, J., Erbacher, J., 2010. Calcareous nannofossils of the Cenomanian/Turonian boundary interval from the Boreal Realm (Wunstorf, northwest Germany). Marine Micropaleontology 74, 38–58.
Linnert, C., Mutterlose, J., Herrle, J.O., 2011a. Late Cretaceous (Cenomanian–Maastrichtian) calcareous nannofossils from Goban Spur (DSDP Sites 549, 551): Implications for the palaeoceanography of the proto North Atlantic. Palaeogeography, Palaeoclimatology, Palaeoecology 299, 507–528.
Linnert, C., Mutterlose, J., Mortimore, R., 2011b. Calcareous nannofossils from Eastbourne (southeastern England) and the paleoceanography of the Cenomanian-Turonian boundary interval. Palaios 26, 298–313.
Luciani, V., Cobianchi, M., 1999. The Bonarelli Level and other black shales of the Cenomanian-Turonian of the northeastern Dolomites (Italy): calcareous nannofossil and foraminiferal data. Cretaceous Research 20, 135–167.
Masse, J.P., Philip, J., 1976. Paléogéographie et tectonique du Crétacé moyen en Provence: révision du concept d'isthme durancien. Revue de Géographie Physique et Géologie Dynamique 18, 49–66.
Melinte-Dobrinescu, M.C., Bojar, A.-V., 2008. Biostratigraphic and isotopic record of the Cenomanian–Turonian deposits in the Ohaba-Ponor section (SW Hateg, Romania). Cretaceous Research 29, 1024–1034.
Miller, K.G., Sugarman, P.J., Browning, J.V., Kominz, M.A., Hernández, J.C., Olsson, R.K., Wright, J.D., Feigenson, M.D., Van Sickel, W., 2003. Late Cretaceous chronology of large, rapid sea level changes: Glacioeustasy during the greenhouse world. Geology 31, 585–588.
Miller, K.G., Wright, J.D., Browning, J.V., 2005. Visions of ice sheets in a greenhouse world. Marine Geology 217, 215–231.
Mitchell, S.F., Carr, I.T., 1998. Foraminiferal response to mid-Cenomanian (Upper Cretaceous) palaeoceanographic events in the Anglo-Paris Basin (Northwest Europe). Palaeogeography, Palaeoclimatology, Palaeoecology 137, 103–125.
Mitchell, S.F., Paul, C.R.C., Gale, A.S., 1996. Carbon isotopes and sequence stratigraphy. In: Howell, J.A., Aitken, J.F. (Eds.), High Resolution Sequence Stratigraphy: Innovations and Applications, Geological Society London Special Publications 104, pp. 11–24.
Moiroud, M., Martinez, M., Deconinck, J.F., Monna, F., Pellenard, P., Riquier, L., Company, M., 2012. High resolution clay mineralogy as a proxy for orbital tuning: Example of the Hauterivian-Barremian transition in the Betic Cordillera (SE Spain). Sedimentary geology 282, 336–346.

Monnet, C., Bucher, H., 2002. Cenomanian (early Late Cretaceous) ammonoid faunas of Western Europe. Part 1: Biochronology (Unitary Associations) and diachronism of datums. Eclogae Geologicae Helvetiae 95, 57–73.
Monnet, C., Bucher, H., Escarguel, G., Guex, J., 2003. Cenomanian (early Late Cretaceous) ammonoid faunas of Western Europe. Part 2: Diversity patterns and the end-Cenomanian anoxic event. Eclogae Geologicae Helvetiae 96, 381–398.
Moore, D.M., Reynolds, R.C., 1997. X-Ray Diffraction and the Identification and Analysis of Clay Minerals, 2nd edition. Oxford University Press, Inc., New York, NY. 400 pp.
Morgan-Jones, M., 1977. Mineralogy of non-carbonate material from the chalk of Berkshire and Oxfordshire, England. Clay Minerals 12, 331–344.
Moriya, K., Wilson, P., Friedrich, O., Erbacher, J., Kawahata, H., 2007. Testing for ice sheets during the mid-Cretaceous greenhouse using glassy foraminiferal calcite from the mid-Cenomanian tropics on Demerara Rise. Geology 35, 615–618.
Mutterlose, J., 1992. Biostratigraphy and palaeogeography of Early Cretaceous calcareous nannofossils. Cretaceous Research 13, 167–189.
Mutterlose, J., 1996. Calcareous nannofossil palaeoceanography of the Early Cretaceous of NW Europe. Mitteilungen aus dem Geologish-Paläontologishen Institut der Universität Hamburg 77, 291–313.
Mutterlose, J., Kessels, K., 2000. Early Cretaceous calcareous nannofossils from high latitudes: implications for palaeobiogeography and palaeoclimate. Palaeogeography, Palaeoclimatology, Palaeoecology 160, 347–372.
Paul, C.R.C., Mitchell, S.F., Marshall, J.D., Leary, P.N., Gale, A.S., Duane, A.M., Ditchfield, P.W., 1994. Palaeoceanographic events in the Middle Cenomanian of Northwest Europe. Cretaceous Research 15, 707–738.
Perch-Nielsen, K., 1985. Mesozoic Calcareous Nannofossils. In: Bolli, H.M., Saunders, J.B., Perch-Nielsen, K. (Eds.), Plankton Stratigraphy. Cambridge University Press, pp. 17–86.
Peybernes, C., Giraud, F., Jaillard, E., Robert, E., Masrour, M., Aoutem, M., Içame, N., 2013. Stratigraphic framework and calcareous nannofossil productivity of the Essaouira-Agadir Basin (Morocco) during the Aptian-EarlyAlbian: comparison with the north Tethyan margin. Cretaceous Research 39, 149–169.
Philip, J., 1978. Stratigraphie et paléoécologie des formations à rudistes du Cénomanien: l'exemple de la Provence. Géologie Méditerranéenne 5, 155–168.
Reboulet, S., 2008. Origination of *Himantoceras* (heteromorphic ammonoids) related to palaeoceanography and climatic changes during the Valanginian. In: 1st International Meeting on Correlation of Cretaceous Micro- and Macrofossils, Vienna (Austria), 16–18 April, 2008. Berichte der Geologischen Bundesanstalt, 74, pp. 89–91.
Reboulet, S., Mattioli, E., Pittet, B., Baudin, F., Olivero, D., Proux, O., 2003. Ammonoid and nannoplankton abundance in Valanginian (early Cretaceous) limestone-marl successions from the southeast of France basin: carbonate dilution or productivity? Palaeogeography, Palaeoclimatology, Palaeoecology 201, 113–139.
Reboulet, S., Giraud, F., Proux, O., 2005. Ammonoid abundance variations related to changes in trophic conditions across the oceanic anoxic event 1d (Latest Albian, SE France). Palaios 20, 121–141.
Reboulet, S., Giraud, F., Colombié, C., Carpentier, A., 2013. Integrated stratigraphy of the Lower and Middle Cenomanian in a Tethyan section (Blieux, southeast France) and correlations with Boreal basins. Cretaceous Research 40, 170–189.
Robaszynski, F., Amédro, F., Foucher, J.C., Gaspard, D., Magniez-Jannin, F., Manivit, H., Sornay, J., 1980. Synthèse biostratigraphique de l'Aptien au Santonien du Boulonnais à partir de sept groupes paléontologiques: foraminifères, nannoplancton, dinoflagellés et macrofaunes. Zonations micropaléontologiques intégrées dans le cadre du Crétacé boréal nord-européen. Revue de micropaléontologie 22, 195–321.
Robaszynski, F., Juignet, P., Gale, A.S., Amédro, F., Hardenbol, J., 1998. Sequence stratigraphy in the Cretaceous of the Anglo-Paris Basin, exemplified by the Cenomanian stage. In: de Graciansky, P.C., Hardenbol, J., Jacquin, T., Vail, P.R. (Eds.), Mesozoic and Cenozoic sequence stratigraphy of European basins, Society of Economists, Palaeontologists and Mineralogists, Special Publications 60, pp. 363–386.
Rodriguez-Lazaro, J., Pascual, A., Elorza, J., 1998. Cenomanian events in the deep western Basque Basin: the Leioa section. Cretaceous Research 19, 673–700.
Roth, P.H., 1981. Mid-Cretaceous calcareous nannoplankton from the Central Pacific: implication for paleoceanography. In: Thiede, J., et al. (Eds.), Initial Reports of the Deep Sea Drilling Project 62, pp. 471–489.
Roth, P.H., 1983. Jurassic and Lower Cretaceous calcareous nannofossils in the western North Atlantic (Site 534): biostratigraphy, preservation, and some observations on biogeography and palaeoceanography. In: Sheridan, R.E., Gradstein, F.M., et al. (Eds.), Initial Reports of the Deep Sea Drilling Project 76, pp. 587–621.
Roth, P.H., 1986. Mesozoic palaeoceanography of the North Atlantic and Tethys oceans. In: Summerhayes, C.P., Schackleton, N.J. (Eds.), North Atlantic palaeoceanography, Geological Society Special Publications, pp. 299–320.
Roth, P.H., Bowdler, J., 1981. Middle Cretaceous nannoplankton biogeography and oceanography of the Atlantic Ocean. In: Warme, J.E., Douglas, R.G., Winterer, E.L. (Eds.), The Deep Sea Drilling Project: a Decade of Progress, Society of Economic Paleontologists and Mineralogists Special Publications 32, pp. 517–546.
Roth, P.H., Krumbach, K.R., 1986. Middle Cretaceous calcareous nannofossil biogeography and preservation in the Atlantic and Indian oceans: implications for paleoceanography. Marine Micropaleontology 10, 235–266.
Rubino, J.L., 1989. Introductory remarks on upper Aptian to Albian silicoclastis/carbonate depositional sequences. In: Ferry, S., Rubino, J.L. (Eds.), Mesozoic eustacy record on western Tethyan margins. Guide-book of the post-meeting field trip in the Vocontian Trough, 25th–28th November 1989. 2ème Congrès Français de Sédimentologie, Lyon, pp. 28–56.
Sauvage, L., 2011. Geochemical clues for oxic to dysoxic conditions during Cretaceous "Oceanic Anoxic Events". Unpublished Thesis. University of Burgundy, 55 pp.
Scholle, P.A., Arthur, M.A., 1980. Carbon isotope fluctuations in Cretaceous pelagic limestones: Potential stratigraphic and petroleum exploration tools. American Association of Petroleum Geologists Bulletin 64, 67–87.
Shannon, C.E., Weaver, W., 1949. The mathematical Theory of Communication. University of Illinois Press, 125 pp.
Sokal, R.R., Rohlf, F.J., 1995. Biometry: The principles and practice of statistics in biological research, 3rd edition. W.H. Freeman, New York. 887 pp.
Środoń, J., 1984. X-ray powder diffraction identification of illitic materials. Clays and clay minerals 32, 337–349.
Środoń, J., Clauer, N., Huff, W., Dudek, T., Banaś, M., 2009. K-Ar dating of the Lower Palaeozoic K-bentonites from the Baltic Basin and the Baltic Shield: implications for the role of temperature and time in the illitisation of smectite. Clay Minerals 44, 361–387.
Stoll, H.M., Schrag, D.P., 2000. High-resolution stable isotope records from the Upper Cretaceous rocks of Italy and Spain: Glacial episodes in a greenhouse planet? Geological Society of America Bulletin 112, 308–319.
Stoll, H.M., Schrag, D.P., 2001. Sr/Ca variations in Cretaceous carbonates: relation to productivity and sea level changes. Palaeogeography, Palaeoclimatology, Palaeoecology 168, 311–336.
Thierstein, H.R., 1980. Selective dissolution of Late Cretaceous and earliest Tertiary calcareous nannofossils: experimental evidence. Cretaceous Research 2, 165–176.
Thiry, M., 2000. Palaeoclimatic interpretation of clay minerals in marine deposits: an outlook from the continental origin. Earth-Science Reviews 49, 201–221.
Thiry, M., Jacquin, T., 1993. Clay mineral distribution related to rift activity, sea-level changes and paleoceanography in the Cretaceous of the Atlantic Ocean. Clay Minerals 28, 61–84.
Thomel, G., 1972. Les Acanthoceratidae cénomaniens des chaînes subalpines méridionales. Mémoire de la Société Géologique de France 116, 1–204.
Thomel, G., 1992. Ammonites du Cénomanien et du Turonien du sud-est de la France. In: Editions Serre Nice, tome1, 422 p, tome 2, 384 pp.
Uramoto, G.-I., Fujita, T., Takahashi, A., Hirano, H., 2007. Cenomanian (Upper Cretaceous) carbon isotope stratigraphy of terrestrial organic matter for the Yezo Group, Hokkaido, Japan. Island Arc 16, 465–478.
Voigt, S., Flögel, S., Gale, A.S., 2004. Midlatitude shelf seas in the Cenomanian-Turonian greenhouse world: Temperature evolution and North Atlantic circulation. Paleoceanography 19. http://dx.doi.org/10.1029/2004PA001015.
Voigt, S., Erbacher, J., Mutterlose, J., Weiss, W., Westerhold, T., Wiese, F., Wilmsen, M., Wonik, T., 2008. The Cenomanian – Turonian of the Wunstorf section – (North Germany): global stratigraphic reference section and new orbital time scale for Oceanic Anoxic Event 2. Newsletters on Stratigraphy 43, 65–89.
Watkins, D.K., 1989. Nannoplankton productivity fluctuations and rhythmically-bedded pelagic carbonates of the Greenhorn Limestone (Upper Cretaceous). Palaeogeography, Palaeoclimatology, Palaeoecology 74, 75–86.
Wilmsen, M., 2003. Sequence stratigraphy and palaeoceanography of the Cenomanian Stage in northern Germany. Cretaceous Research 24, 525–568.
Wilmsen, M., 2007. Integrated stratigraphy of the upper Lower – lower Middle Cenomanian of northern Germany and southern England. Acta Geologica Polonica 57, 263–279.
Wilmsen, M., Mosavinia, A., 2011. Phenotypic plasticity and taxonomy of *Schloenbachia varians* (J. Sowerby, 1817) (Cretaceous Ammonoidea). Paläontologische Zeitschrift 85, 169–184.
Wilmsen, M., Niebuhr, B., Hiss, M., 2005. The Cenomanian of northern Germany: facies analysis of a transgressive biosedimentary system. Facies 51, 242–263.
Wilmsen, M., Wood, C.J., Niebuhr, B., Zawischa, D., 2007. The fauna and palaeoecology of the Middle Cenomanian *Praeactinocamax primus* Event from the type-locality (Wünstorf quarry, northern Germany). Cretaceous Research 28, 428–460.
Wray, D.S., 1995. Origin of clay-rich beds in Turonian chalks from Lower Saxony, Germany – a rare-earth element study. Chemical Geology 119, 161–178.
Wray, D.S., 1999. Identification and long-range correlation of bentonites in Turonian-Coniacian (Upper Cretaceous) chalks of Northwest Europe. Geological Magazine 136, 361–371.
Wray, D.S., Kaplan, U., Wood, C., 1995. Tuff-Vorkommen und ihre Bio-und Eventstratigraphie im Turon des Teutoburger Waldes, der Egge und des Haarstrangs. Geologie und Paläontologie in Westfalen 37, 3–53.
Wright, C.W., Calloman, J.H., Howarth, M.K., 1996. Cretaceous Ammonoidea. In: Kaesler, R.L. (Ed.), Treatise on Invertebrate Palaeontology, Part L, Mollusca 4. Geological Society of America, University of Kansas, Boulder and Lawrence, 362 pp.